

CHARACTERISTICS AND PREDICTION OF THE LOW TEMPERATURE INDIRECT
TENSILE STRENGTHS OF MICHIGAN ASPHALT MIXTURES

By

Michael Krcmarik

A THESIS

Submitted to
Michigan State University
in partial fulfillment of the requirements
for the degree of

Civil Engineering – Master of Science

2013

ABSTRACT

CHARACTERISTICS AND PREDICTION OF THE LOW TEMPERATURE INDIRECT TENSILE STRENGTHS OF MICHIGAN ASPHALT MIXTURES

By

Michael Krcmarik

Thermal cracking is the predominant flexible pavement distress in northern climates, causing transverse cracking perpendicular to the direction of traffic. The indirect tensile (IDT) strength test is currently the most widely used method to characterize thermal cracking susceptibility and is an input to the Pavement ME Design software (formerly known as the Mechanistic- Empirical Design Guide (MEPDG)). In Pavement ME Design when laboratory IDT strength testing data is not available to designers it is predicted using mixture volumetrics and performance grade (PG) of the binder. The purpose of this research is to examine the IDT strength characteristics of flexible pavement mixtures commonly used by the Michigan Department of Transportation (MDOT) and to develop improved prediction methods for IDT strength. Laboratory testing of 62 unique MDOT mixtures showed Pavement ME Design software generally over predicted IDT strength. Three models were developed to improve the accuracy of IDT strength prediction. The first model consists of local calibration of the current IDT strength Pavement ME Design predictive model for MDOT mixes. The second model consists of a new statistical model developed based on job mix information to predict low temperature IDT strength. The third model consists of an artificial neural network developed to predict low temperature strength from job mix information. All three models showed increased prediction performance when compared to Pavement ME Design IDT strength prediction. With these models, a more accurate low temperature prediction of IDT strength is available to pavement designers in Michigan using readily available job mix information.

TABLE OF CONTENTS

LIST OF TABLES	v
LIST OF FIGURES	vi
1. INTRODUCTION	1
1.1 Objective.....	3
1.2 Outline.....	3
2. LITERATURE REVIEW	4
2.1 Motivation	4
2.2 Background of the Indirect Tensile Strength Test	4
2.3 Current Indirect Tensile Strength Testing Procedure.....	7
2.4 Calculation of Indirect Tensile Strength According to AASHTO T-322	10
2.5 Calculation of Indirect Tensile Strength without Deformation Monitoring.....	11
2.6 Determination of Fracture Work from Indirect Tensile Strength Testing.....	12
2.7 Relevance of Indirect Tensile Strength to Pavement ME Design.....	14
2.8 Pavement ME Design IDT Strength Prediction	16
2.9 Factors Affecting Mixture Indirect Tensile Strength	17
3. METHODS	19
3.1 Introduction	19
3.2 Mixtures Used	19
3.3 Specimen Preparation.....	23
3.4 Indirect Strength Testing Procedures	24
3.4.1 Testing Temperature.....	24
3.4.2 Use of LVDTs	24
3.4.3 Environmental Chamber.....	25
4. RESULTS OF LABORATORY INDIRECT TENSILE TESTING	27
4.1 Indirect Tensile Strength of Michigan Mixtures	27
4.2 Fracture Work of Michigan Mixtures	30
4.3 MDOT Mix Designation and IDT Strength	38
4.4 Superpave PG and IDT Strength.....	40
4.5 Warm Mix Asphalt IDT Properties.....	44
5. INDIRECT TENSILE STRENGTH PREDICTION MODELS.....	47
5.1 Introduction to Indirect Tensile Strength Prediction for Pavement ME Design.....	47
5.2 Model Evaluation	49
5.3 Local Calibration of Pavement ME Design Strength Prediction Model.....	50
5.4 Linear Strength Prediction Model	55
5.5 Artificial Neural Network Prediction Model	62
5.5.1 Structure of the IDT Strength ANN	63
5.5.2 Overview of IDT Strength Prediction with the ANN.....	63

5.5.2 Training of the IDT Strength ANN	65
5.5.3 Testing of the IDT Strength ANN	68
6. CONCLUSIONS AND RECOMMENDATIONS	70
APPENDICES	72
APPENDIX A: MIX PROPERTIES AND VOLUMETRICS OF MIXTURES TESTED	73
APPENDIX B: IDT STRENGTH, FRACTURE WORK, AND VOLUMTERICS OF SPECIMENS TESTED	85
REFERENCES	102

LIST OF TABLES

Table 1 HMAs tested for IDT strength.....	20
Table 2 HMAs tested for IDT strength (GGSP and LVSP Mixtures)	22
Table 3 HMAs tested for IDT strength (SUPERPAVE) – Mixtures that do not follow MDOT specifications but are permitted to be used.....	23
Table 4 HMAs tested for IDT strength (GGSP and LVSP Mixtures) - Mixtures that do not follow MDOT specifications but are permitted to be used	23
Table 5 Summary of IDT strength values for the State of Michigan asphalt mixtures	28
Table 6 Summary of total work values for the State of Michigan asphalt mixtures	31
Table 7 Summary of pre fracture work values for the State of Michigan asphalt mixtures.....	33
Table 8 Summary of post fracture work values for the State of Michigan asphalt mixtures	35
Table 9 Binder and Mixture Properties of 36 MDOT Mixtures used in Michigan Calibration of the Pavement ME Design Strength Prediction Model Developed by Witczak	51
Table 10 Comparison of the original and Michigan calibrated Pavement ME Design IDT strength Model Calibration Coefficients.....	52
Table 11 Comparison of model performance evaluation parameters measured for Original Pavement ME Design and Calibrated IDT strength prediction models for 36 MDOT asphalt mixtures.....	55
Table 12 MDOT JMF parameters found to be significantly correlated with measured IDT strength using a Pearson Correlation analysis. Correlation significance, either at the .01 or .05 level, and the relationship of the parameter, either positive (+) or negative (-), is also listed.....	56
Table 13 Comparison of performance criteria for the original Pavement ME Design and linear IDT strength prediction models for commonly used MDOT asphalt mixtures	61
Table 14 Overview of specimens used and correlation coefficients for each stage of IDT ANN development.....	69
Table 15 Mixture properties and volumetrics of mixtures tested	74
Table 16 IDT Strength, Fracture Work, and Air Voids of Specimens Tested.....	86

LIST OF FIGURES

Figure 1 Examples of typical thermal cracking distress in flexible pavements evidenced by transverse cracking in the direction perpendicular to travel. For interpretation of the references to color in this and all other figures, the reader is referred to the electronic version of this thesis. ...	1
Figure 2 Development of stress in a diametrically loaded specimen during the IDT strength test	5
Figure 3 IDT strength test specimen at failure.....	6
Figure 4 Overview of the IDT strength specimen fabrication and testing process.....	9
Figure 5 Typical (Y-X) versus time curve depicting first peak time	10
Figure 6 Typical IDT stress versus strain curve depicting pre and post energy	13
Figure 7 IDT test system consisting of an axial loading device with external environmental chamber.....	26
Figure 8 Total fracture work versus IDT strength relationship	38
Figure 9 Laboratory measured IDT strength for MDOT Mix ESAL designation categories for leveling and top course pavement layers	39
Figure 10 Laboratory measured total fracture work for MDOT Mix ESAL designation categories for leveling and top course pavement layers.....	40
Figure 11 IDT strength versus Low Temperature PG relationship.....	41
Figure 12 IDT strength for high PG characterization of Michigan asphalt mixtures	41
Figure 13 Fracture work for low temperature Superpave PG characterization of Michigan asphalt mixtures.....	42
Figure 14 Fracture work for high temperature Superpave PG characterization of Michigan asphalt mixtures	43
Figure 15 IDT strength for comparable WMA and HMA mixtures.....	44
Figure 16 IDT fracture work for comparable WMA and HMA mixtures	45
Figure 17 IDT post fracture work for comparable WMA and HMA mixtures	46

Figure 18 Effect of IDT strength input in Pavement ME Design Level 3 thermal cracking analysis for a 4", PG 58-22 flexible pavement constructed in Detroit, Michigan.	48
Figure 19 Original Pavement ME Design IDT Strength Model for 36 MDOT mixtures with respect to the LOE	53
Figure 20 Michigan Calibrated Pavement ME Design IDT Strength Model for 36 MDOT mixtures with respect to the LOE	54
Figure 21 IDT strength predicated by Pavement ME Design software versus laboratory measured IDT strength for commonly used State of Michigan asphalt mixtures	59
Figure 22 IDT strength predicated during calibration by newly developed linear model versus laboratory measured IDT strength for commonly used State of Michigan asphalt mixtures	60
Figure 23 IDT strength predicated during testing by newly developed linear model versus laboratory measured IDT strength for commonly used State of Michigan asphalt mixtures	60
Figure 24 IDT strength predicated for all specimens by newly developed linear model versus laboratory measured IDT strength for commonly used State of Michigan asphalt mixtures	61
Figure 25 Structure of the ANN model developed for prediction of IDT strength for Michigan asphalt mixtures	63
Figure 26 Reduction in mean squared error of laboratory measured and ANN predicted IDT strength values during training, validation, and testing stages of ANN development.....	66
Figure 27 ANN predicted IDT strength versus measured IDT strength (base 10) for the training, validation, testing, and all data used in ANN development.....	67
Figure 28 ANN Predicated versus measured IDT strength values for all mixtures used in ANN development.....	68

1. INTRODUCTION

Thermal cracking is the predominant pavement distress in the northern United States and Canada. At low temperatures, cooling of a flexible pavement causes contraction of the aggregate and asphalt binder, creating thermal stresses which manifest as transverse cracking perpendicular to the direction of travel (Figure 1). Thermal cracking leads to additional pavement deterioration mechanisms including water seeping into the base/subbase, pumping, frost heave, and ultimately deterioration of the road leading to premature maintenance.



Figure 1 Examples of typical thermal cracking distress in flexible pavements evidenced by transverse cracking in the direction perpendicular to travel. For interpretation of the references to color in this and all other figures, the reader is referred to the electronic version of this thesis.

The identification and evaluation of mix design factors than can increase thermal cracking resistance is of extreme interest to state agencies seeking to improve pavement performance. The low temperature indirect tensile (IDT) strength is one measure of an asphalt mixture's resistance to thermal cracking and is measured by the IDT strength test. The IDT strength test is currently the most widely used thermal cracking mixture characterization method.

The low temperature IDT strength test is conducted by applying displacement controlled loading along the direction of diameter in a cylindrical specimen until failure. The stress at failure is taken as the low temperature IDT strength. Low temperature IDT strength is directly related to the expected thermal cracking pavement performance in the field. Based on this concept the Pavement ME Design software (i.e., M-E PDG) utilizes semi-mechanistic and semi-empirical models to predict pavement distresses over time, such as thermal cracking.

As a result of research under NCHRP Project 1-37A, the Pavement ME Design software is the most recently developed design guide for newly constructed and rehabilitated pavement designs. The Pavement ME Design software requires traffic, climate, and material inputs to predict pavement distresses and accurate measurement of these inputs is necessary for successful prediction. For thermal cracking prediction in flexible pavements, the Pavement ME Design software requires material inputs of mixture IDT strength and creep compliance values to predict thermal cracking per unit length over time. The IDT strength and creep compliance characterization of the asphalt mixture is required for Levels 1, 2, and 3. Inputs into the Pavement ME Design are classified according to a three level system (Levels 1, 2, and 3), which allow pavement engineers to select the level of design accuracy. A Level 1 analysis requires the most detailed characterization of material inputs and can generally be thought to predict pavement distresses most accurately. A Level 3 analysis requires the least detailed characterization of material inputs; as a result the accuracy of the distress predictions can be low. Many state transportation agencies, including the Michigan Department of Transportation (MDOT), do not have testing programs to measure the required Pavement ME Design Level 1 material inputs for thermal cracking analysis and they are instead predicted by Pavement ME Design using predictive equations at the expense of accuracy.

1.1 Objective

The first objective of this study was to characterize the IDT strength and fracture work of asphalt mixtures commonly used in the State of Michigan. It is important to understand the low temperature fracture properties and if they can be predicted from or are related to current pavement design frameworks, such as Superpave Performance Grading or MDOT mix designation.

The second objective was to examine the accuracy of the predictive equations used by the Pavement ME Design software in predicting low temperature IDT strength and develop improved prediction equations/models if necessary. This is important for accurate prediction of asphalt thermal cracking distress and subsequently successful implementation of the Pavement ME Design software by MDOT.

1.2 Outline

This thesis is organized as follows: Chapter 2 presents a literature review on the background of the IDT creep and strength tests and prediction of IDT strength in Pavement ME Design software. Second, a discussion on the relevance of IDT strength to the Pavement ME Design software and how it is used in thermal cracking prediction is given. Finally, Chapter 2 also reviews current research on mix design factors and volumetrics influencing IDT strength. Chapter 3 presents the materials used in this research and the testing protocol followed. Chapters 4 and 5 present the results of the IDT strength laboratory testing and development of IDT strength predictive models, respectively. Chapter 6 presents the conclusions of this study and recommendations for future work.

2. LITERATURE REVIEW

2.1 Motivation

Thermal cracking is the predominant asphalt pavement distress in northern climates such as the State of Michigan. As the Pavement ME Design becomes state of the practice for the design of new and rehabilitated pavements it is in the best interest of transportation agencies to accurately characterize material inputs in order to successfully predict pavement distresses such as thermal cracking. Review of literature on asphalt mixtures used in the State of Michigan showed a need for low temperature mixture characterization for use in pavement design. Additionally preliminary analysis of Pavement ME Design IDT strength prediction showed poor prediction performance for Michigan mixtures. This study aims to characterize the low temperature strength properties of Michigan asphalt mixtures. Secondly this study aims to predict these low temperature strength properties. Accurate prediction of material properties such as IDT strength is important for successful thermal cracking distress prediction and subsequent successful implementation of the Pavement ME Design software.

2.2 Background of the Indirect Tensile Strength Test

A material's IDT strength is a measure of its tensile strength when loaded diametrically across a circular specimens' cross-section. Figure 2 illustrates the loading scheme and resulting stress distribution within the IDT strength test sample.

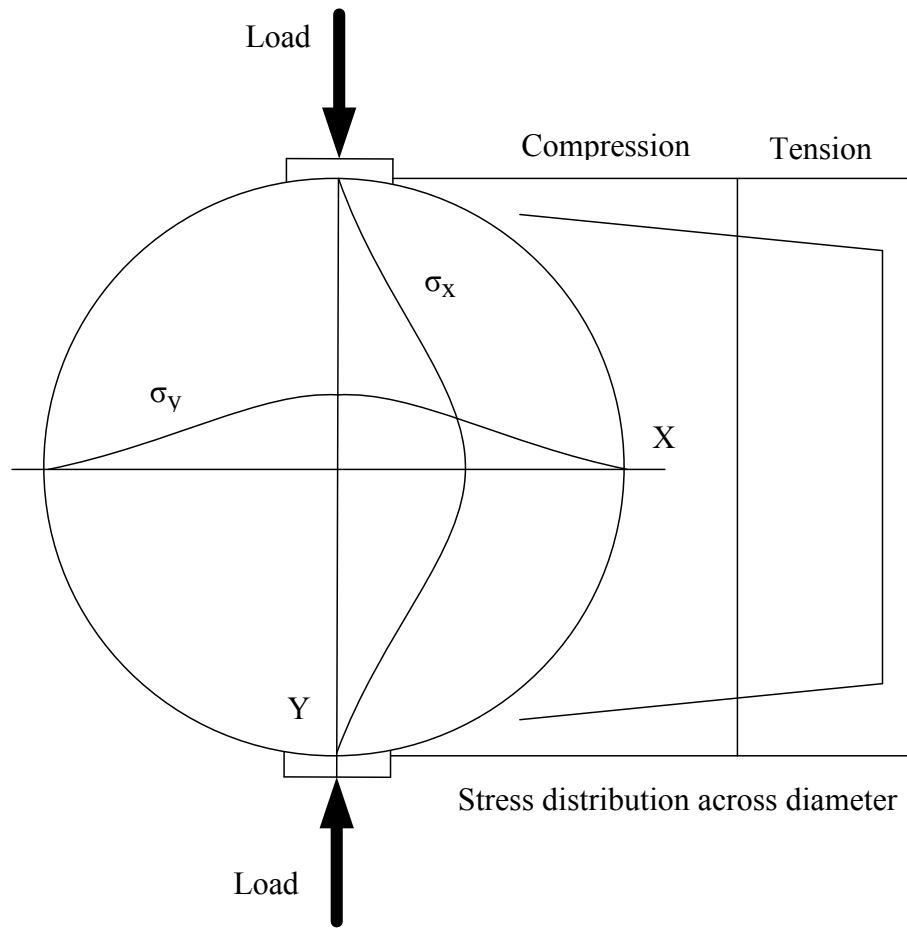


Figure 2 Development of stress in a diametrically loaded specimen during the IDT strength test

Loading applied along the circular specimens' diameter causes tensile forces to develop perpendicular to the direction of loading, ultimately resulting in a tensile failure (Figure 3). The IDT strength test was first used to determine the tensile strength of wood and rock materials in what is commonly known as the Brazilian Test [26]. In 1943 Carneiro [13] applied the IDT strength test to concrete and it is still used as the primary method to determine concrete tensile strength today. In the early 1990's work began by Roque [8] to apply the IDT test to asphalt mixtures and as a result the first procedure for low temperature IDT creep and strength

characterization of asphalt mixtures was developed under the first Strategic Highway research Program (SHRP) [7][8]. As a result of this work the procedure was then codified as an AASHTO standard, AASHTO T-322, “Standard Method of Test for Determining the Creep Compliance and Strength of Hot-Mix Asphalt (HMA) Using the Indirect Tensile Test Device” [1]. In the late 1990’s the IDT strength test underwent further examination by the Federal Highway Administration (FHWA) during the development of Superpave mix design protocol. Due to its accuracy and durability, the IDT strength and creep test was identified as a *simple performance test* for low temperature cracking in HMA mix design. The IDT strength and creep was then also selected as a *materials characterization test* in NCHRP Project 1-37A due to its ability to predict a mixture’s resistance to thermal cracking as evidenced by its good correlation to field thermal cracking data [10].



Figure 3 IDT strength test specimen at failure

Today the IDT strength test is still the most widely used strength test to characterize a mixture's resistance to thermal cracking. Other tests exist to characterize the thermal cracking resistance of asphalt mixtures each with their own advantages and disadvantage and include the Thermal Stress Restrained Specimen Test (TSRST) [21], Semi-Circular Bend (SCB) Test [24], Modified IDT, and Disk-Shaped Compact Tension (DCT) Test [27]. These methods also measure mixture tensile strength to characterize thermal cracking resistance, but differ mostly in specimen geometry, deformation monitoring methods, and loading application in an attempt to rectify perceived shortcomings in the IDT creep and strength test [27]. Yet currently the IDT creep and strength tests are still considered the most promising parameters for predicting the low temperature performance of asphalt mixtures [10].

2.3 Current Indirect Tensile Strength Testing Procedure

The standard test method for the IDT strength is the AASHTO T-322 “Determining the Creep Compliance and Strength of Hot-Mix Asphalt (HMA) Using the Indirect Tensile Test Device.” The AASHTO T-322 contains detailed procedures to determine tensile creep compliance, tensile strength, and Poisson's ratio of an HMA mixture [1]. The summary of the method to determining the tensile strength, commonly known as the IDT strength, is as follows: Bulk laboratory molded specimens are compacted from loose mixture in a Superpave Gyrotory Compactor (SGC). Cylindrical specimens are then cut from the SGC compacted specimens to a diameter of 150 ± 9 mm and to a height of 38 to 50 mm (Figure 4). Bulk Specific Gravity and air voids of each specimen are determined and only specimens meeting air voids of $7 \pm .5\%$ are selected for testing. Once specimens are fabricated to geometric and volumetric criteria two linear variable differential transducers (LVDTs) are attached to each of the two specimen's faces with the use of mounting gauges and epoxy (Figure 4). Specimens are then conditioned in an

environmental chamber at the test temperature for 3 ± 1 hours prior to testing. A test temperature of 0°C or less is used for thermal cracking analysis, however if the analysis is used for Superpave design, test temperatures of 0, -10, and -20°C are recommended.

After conditioning, the specimen is placed into a testing frame located inside an Indirect Tensile Test System (Figure 4, Step 3). The IDT Test System consists of an axial loading device, environmental chamber, and a control and data acquisition system. At the test temperature, load is applied to the specimen at a rate of 12.5 mm of vertical ram movement per minute. During load application vertical and horizontal deformations on both faces of the specimen and the load magnitude are recorded. Displacement controlled loading is applied until the load starts to decrease, at which point strength test is complete. The desired failure mode consists of a vertical crack running along the length of the specimen's diameter in line with the direction of loading (Figure 3 and Figure 4).



Step 1) Bulk specimens are compacted from loose mixture samples using the SGC



Step 2) Compacted specimens are cut to dimension and volumetric properties measured



Step 3) Specimens are mounted with LVDTs and conditioned at the testing temperature



Step 4) Load is applied until failure (LVDTs removed for display purposes)

Figure 4 Overview of the IDT strength specimen fabrication and testing process

2.4 Calculation of Indirect Tensile Strength According to AASHTO T-322

AASHTO T-322 defines failure as the point when vertical deformations (Y) minus horizontal deformations (X) (as measured by the LVDTs) reach a maximum value. This time is called first peak time and the load at this time is called the first failure load (Figure 5).

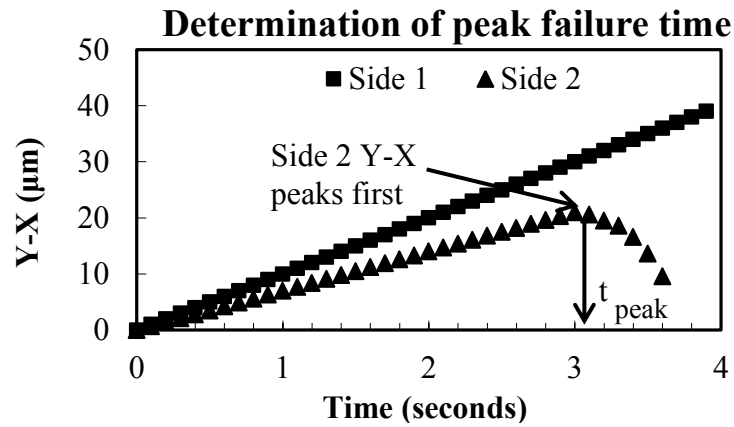


Figure 5 Typical (Y-X) versus time curve depicting first peak time

The failure load is then used along with specimen geometry to determine the tensile strength.

The procedure is as follows.

1. Determine failure time, t_f for both faces of the specimen, defined as the time when vertical deformation minus horizontal deformation reaches a maximum value. Take the shortest t_f .
2. Obtain the failure load, P_f at time t_f .
3. Calculate the IDT strength, S_t .

$$S_t = \frac{2 \times P_f}{\pi \times b_n \times D_n} \quad (1)$$

Where,

b_n = average thickness of the specimen

D_n = average diameter of the specimen

2.5 Calculation of Indirect Tensile Strength without Deformation Monitoring

Under NCHRP 530 report [10] AASHTO T-322 was thoroughly examined in an effort to first validate and secondly determine possible improvements to the test. One of the suggested improvements proposed in NCHRP 530 report was IDT strength testing without the use of LVDTs to monitor deformations. LVDTs were initially incorporated into AASHTO T-322 because the precise moment of failure during the IDT test is difficult to determine due to the often slow specimen failure and ability of the specimen to carry significant load even after cracks become visible along the specimen face. Despite the accuracy and precision of the exact failure moment determination with the LVDTs testing at state agencies, the FHWA, and regional Superpave Centers reported feasibility issues with using the LVDTs. LVDTs were found to be difficult to keep in place and due to the sometimes explosive nature of specimen failure, the expensive and delicate LVDTs were at risk to be damaged during testing, potentially jeopardizing overall reliability and accuracy of the IDT strength test. As a result of feedback from testing centers, an empirical relationship was found between the true (corrected) and uninstrumented (uncorrected) strength values and evaluated in NCHRP 530 report [10] (Equation 2). The empirical equation relating corrected and uncorrected IDT strength values was found to be accurate and able to predict true strength reasonably well from uninstrumented IDT strength as compared to LVDT instrumented testing. For practical purposes the IDT strength testing that serves at the basis of this thesis did not employ LVDTs during testing and Equation

2, developed by NCHRP-530 researchers, was used to estimate the true strength (instrumented) from the uninstrumented strength. The strength at maximum load is termed the uncorrected strength (Equation 2).

$$\text{True Tensile Strength (psi)} = [0.781 \times \text{Uncorrected IDT Strength (psi)}] + 38 \quad (2)$$

2.6 Determination of Fracture Work from Indirect Tensile Strength Testing

The IDT strength test can also be used to measure a mixture's fracture energy [22] [25] and fracture work [39]. Fracture energy of a mixture is defined as the area under the stress versus strain curve while similarly fracture work is the area under the load versus horizontal displacement curve. Total fracture energy consists of pre-peak energy (fracture energy measured until failure), and post-peak fracture energy (fracture energy measured after failure) depicted in Figure 6 [40].

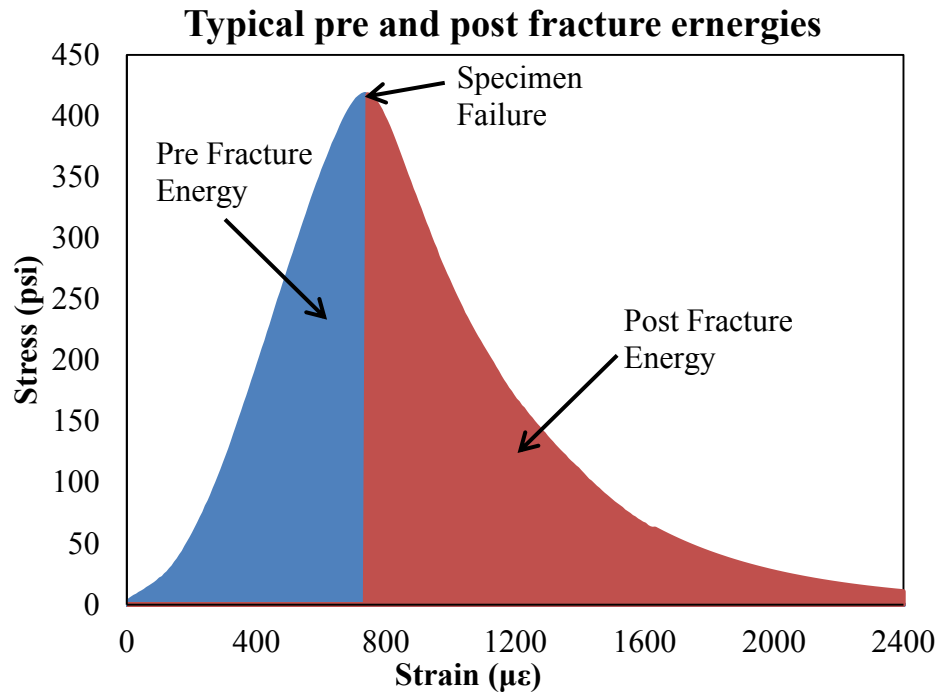


Figure 6 Typical IDT stress versus strain curve depicting pre and post energy

Pre-peak fracture energy is associated with crack initiation while post-peak fracture energy is associated with crack propagation [40]. High pre-peak fracture energy would be indicative of greater resistance to thermal cracking initiation, while high post-peak fracture energy would be associated with a lower rate of thermal cracking propagation. A mixture high in fracture energy, pre or post, would generally be expected to exhibit lower rates of thermal cracking compared to a mixture with lower fracture energy.

In this thesis fracture work was used to characterize mixture thermal cracking resistance instead of fracture energy. Fracture work measured by the IDT test has been shown to correlate well with field performance whereas fracture energy has been shown not to correlate well with field performance [39]. This is in part due to fracture work's ability to capture the entire post-peak behavior whereas fracture energy often cannot due to limits in the range of LVDT

measurements. Another advantage of fracture work is the elimination of LVDT instrumentation during testing. Vertical ram movement has been shown to be no different than LVDT measured horizontal displacement [39]. This enables rapid testing and eliminates LVDT damage. For these reasons the use of fracture work was used in this thesis as an additional method to characterize thermal cracking susceptibility of Michigan mixtures.

2.7 Relevance of Indirect Tensile Strength to Pavement ME Design

Pavement ME Design is the latest pavement design guide developed as a result of research completed under NCHRP 1-37A. In the Pavement ME Design distresses are predicted over a design period based on material properties, climate, traffic, and design geometry. Pavement engineers input a design pavement cross section and can predict pavement distresses over time and modify their design accordingly.

Pavement ME Design predicts thermal cracking in flexible pavements using the Thermal Cracking (TC) Model first developed by Hiltunen and Roque [17] [36]. The TC Model takes into account material inputs, climate, and design geometry to predict the amount of thermal cracking per length of pavement over time. For example, a typical MDOT HMA pavement constructed in Northern Michigan may be predicted to exhibit thermal cracking distress of 500 feet per mile after 20 years. The amount of thermal cracking in the TC Model is predicted in three steps. First thermal stress distribution due to cooling is calculated. Second, crack propagation is modeled. And lastly the amount of cracking visible on the pavement surface is calculated [28] [40]. Mixture IDT strength is used as an input into the calculation of crack propagation portion of the TC Model and is discussed subsequently.

Crack growth rate in the TC Model is governed using the Paris Law, given by the following equation [28]:

$$\Delta C = A(\Delta K)^n \quad (3)$$

where:

ΔC = change in crack length

ΔK = change in the stress intensity factor

A, n = regression parameters

The change in the stress intensity factor, ΔK , is determined through a subroutine program called CRACKTIP, a finite element program used to calculate the stress at the tip of a single vertical thermal crack [17]. A and n are regression parameters originally derived by Schapery [35] for nonlinear viscoelastic materials and related to creep compliance, IDT strength, and fracture work [35]. A and n can be empirically related to mixture strength, IDT strength, and creep compliance through the following relationships [35].

$$\log A = 4.389 - 2.52 \times \log(E \times \sigma_m \times n) \quad (4)$$

Where:

E = mixture stiffness, psi

σ_m = mixture IDT strength, psi

$$n = 0.8 \times \left(1 + \frac{1}{m}\right)$$

m = slope of the linear portion of the log compliance-log time relationship determined from the IDT creep test

In summary, the IDT strength is directly used as an input into calculating the A parameter and used in calculation of crack propagation in the Pavement ME Design TC Model. The accuracy of the thermal cracking model is therefore directly dependent on the accuracy of the models used for estimating creep compliance and tensile strength, which is the subject of this thesis.

2.8 Pavement ME Design IDT Strength Prediction

In the TC Model subroutine of Pavement ME Design, IDT strength at -10°C is a direct input in Level 1 and Level 2 analysis, often measured by universities or private testing facilities as most state agencies do not have their own testing programs in place. For Level 3 analysis IDT strength at -10°C is still required but is estimated from the binder PG and mixture volumetrics. Initially IDT strength was predicated based solely on binder PG, i.e. any mixture containing PG 58-28 would have an IDT strength of 400 psi while any mixture containing PG 64-34 would have an IDT strength of 475 psi. This initial predictive model was found to provide a biased estimate and high variance in predicting IDT strength [6]. Final modification and revision of the TC Model by Witczak et al [6] under NCHRP 9-19 revised the IDT strength prediction subroutine of the TC Model based on correlations with PG and volumetric and mixture properties [6]. IDT strength was found to correlate well with air voids, voids filled with asphalt (VFA), the Penetration at 77°F , and the A intercept of the RTFO conditioned binder temperature-viscosity relationship. Based on these relationships, the following empirical equation was developed.

$$S_t = 7416.712 - 114.016V_a - 0.304V_a^2 - 122.592VFA + 0.704VFA^2 + 405.71\log(Pen_{77}) - 2039.296\log(ARTFO) \quad (5)$$

Where:

S_t = Indirect tensile strength at -10°C (psi)

V_a = Air Voids, %

VFA = Voids Filled with Asphalt, %

Pen_{77} = Penetration at 77°F

$ARTFO$ = Intercept of RTFO conditioned binder Viscosity-Temperature relationship

Binder material parameter $ARTFO$ is not directly input into Pavement ME software, instead it is predicted from binder PG. Pen_{77} is also not required and is predicted from binder PG.

Global calibration of the IDT strength subroutine in the TC Model was completed using 31 data points. Goodness of fit statistics S_e/S_y (standard error of estimate/standard deviation), and correlation coefficient (R^2) were 0.68 and 0.62, respectively [6].

2.9 Factors Affecting Mixture Indirect Tensile Strength

Much work has been done on low temperature characterization of asphalt binder, while less work has been done on low temperature characterization of the asphalt mixture. Relatively few studies have examined the effects of mixture properties and volumetric influences on the low temperature IDT strength. Because of the use of IDT strength in thermal cracking resistance

characterization in Pavement ME Design it is important to understand the mixture and volumetric properties that affect IDT strength and thus directly impact thermal cracking susceptibility. NCHRP 530 reported IDT strength values correlated well with voids filled with asphalt (VFA). Low temperature cracking research by Zborowsk and Kaloush [40] showed that crumb rubber modified mixtures exhibited a lower IDT strength and higher fracture energy values as compared to conventional HMA mixtures. In 2011 the National Asphalt Pavement Association in their Warm Mix Asphalt (WMA) best practices report hypothesized that as a result of lower production and placement temperatures WMA mixtures would be softer and thus lead to greater resistance to thermal cracking regardless of their respective WMA additive [16]. Li et al. [25] examined the effect of binder type, binder, modifier, aggregate type, asphalt content, and air voids on the fracture work and fracture toughness of 28 asphalt mixtures as measured by the IDT strength test. Aggregate type, air voids, and high PG for a constant PG low limit were found to have a significant impact on both fracture work and toughness, while an increase in percent binder was not found to be a significant factor. Fracture work was found to increase as test temperature increased while fracture toughness was found to decrease as test temperature increases [25]. In a 2011 study on the effect of Reclaimed Asphalt Pavement (RAP) on IDT strength values Huang et al. reported that generally increasing the percentage of RAP in an HMA mixture resulted in greater IDT strengths and lower toughness indices as did increasing the long term aging of a mixture [18].

3. METHODS

3.1 Introduction

This study was part of a larger comprehensive research effort to characterize asphalt mixtures commonly used in the State of Michigan, for MDOT implementation of Pavement ME Design. In this study 62 different asphalt mixtures were characterized using the IDT strength test to determine IDT strength, total fracture work, pre-peak fracture work, and post-peak fracture work.

3.2 Mixtures Used

Mixtures used in this study consisted of 58 unique HMA and 4 unique WMA mixtures obtained as loose mixture samples by MDOT personal from MDOT pavement projects across the State of Michigan (North, Grand, Bay, Southwest and University Regions, Metro Region, and Superior Region). Mix design volumetrics and aggregate gradations were also provided by MDOT for each mixture. A description of mixtures tested in this thesis is shown in Table 1 through Table 4, where mixtures tested are highlighted in grey.

Table 1 HMAs tested for IDT strength

	Mix No:	2		3		3		4		5	
	Layer:	Base		Base		Leveling		Leveling/Top		Top	
	Mix Type	Binder PG	HMA#	Binder PG	HMA#	Binder PG	HMA#	Binder PG	HMA#	Binder PG	HMA#
<i>North, Grand, Bay, Southwest and University Regions (NGBSU)</i>											
M	E30	64-22	1	64-22	2A	70-28P	3	70-28P	4	70-28P	5
HS	E30	64-22	1	64-22	2B	76-28P	6	76-28P	7	76-28P	8
M	E50	64-22	9	64-22	10	70-28P	11	70-28P	12	70-28P	13
HS	E50	64-22	9	64-22	10	76-28P	14	76-28P	15	76-28P	16
M	E10	58-22	17	58-22	18A	64-28	19	64-28	20	64-28	21
HS	E10	58-22	17	58-22	18B	70-28P	22	70-28P	23	70-28P	24

Table 1 (cont'd)

	x N	2		3		3		4		5			
		Layer:		Base		Base		Leveling		Leveling/Top		Top	
		Mix Type	Binder PG	HMA#	Binder PG	HMA#	Binder PG	HMA#	Binder PG	HMA#	Binder PG	HMA#	
<i>North, Grand, Bay, Southwest and University Regions (NGBSU)</i>													
M	E3	58-22	25	58-22	26A	64-28	27	64-28	28	64-28	29		
HS	E3	58-22	25	58-22	26B	70-28P	30	70-28P	31	70-28P	32		
M	E03	58-22	33	58-22	34	58-28	35	58-28	36	58-28	37		
HS	E03	58-22	33	58-22	34	64-28	38	64-28	39	64-28	40		
M	E1	58-22	41	58-22	42	58-28	43	58-28	44	58-28	45		
HS	E1	58-22	41	58-22	42	64-28	46	64-28	47	64-28	48		
<i>Metro Region</i>													
M	E30	64-22	1	64-22	2A	70-22P	89	70-22P	90	70-22P	91		
HS	E30	64-22	1	64-22	2B	76-22P	92	76-22P	93	76-22P	94		
M	E50	64-22	9	64-22	10	70-22P	95	70-22P	96	70-22P	97		
HS	E50	64-22	9	64-22	10	76-22P	98	76-22P	99	76-22P	100		
M	E10	58-22	17	*58-22	18A	64-22	101	64-22	102	64-22	103		
HS	E10	58-22	17	58-22	18B	70-22P	104	70-22P	105	70-22P	106		
M	E3	58-22	25	58-22	26A	64-22	107	64-22	108	64-22	109		
HS	E3	58-22	25	58-22	26B	70-22P	110	70-22P	111	70-22P	112		
M	E03	58-22	33	58-22	34	58-22	113	58-22	114	58-22	115		
HS	E03	58-22	33	58-22	34	64-22	116	64-22	117	64-22	118		
M	E1	58-22	41	58-22	42	58-22	119	58-22	120	58-22	121		
HS	E1	58-22	41	58-22	42	64-22	122	64-22	123	64-22	124		
<i>Superior Region</i>													
M	E10	58-28	53	58-28	54	58-34	55	58-34	56	58-34	57		
HS	E10	58-28	53	58-28	54	64-34P	58	64-34P	59	64-34P	60		
M	E3	58-28	61	58-28	62	58-34	63	58-34	64	58-34	65		
HS	E3	58-28	61	58-28	62	64-34P	66	64-34P	67	64-34P	68		
M	E03	58-28	69	58-28	70	58-34	71	58-34	72	58-34	73		
HS	E03	58-28	69	58-28	70	64-34P	74	64-34P	75	64-34P	76		

Table 1 (cont'd)

		Mix No:		2		3		3		4		5	
		Layer:		Base		Base		Leveling		Leveling/Top		Top	
		Mix Type:		Binder PG	HMA#	Binder PG	HMA#	Binder PG	HMA#	Binder PG	HMA#	Binder PG	HMA#
<i>Superior Region</i>													
M	E1	58-28	77	58-28	78	58-34	79	58-34	80	58-34	81		
HS	E1	58-28	82	58-28	83	64-34P	84	64-34P	85	64-34P	86		
Note: M=Mainline, HS=High Stress													

Table 2 HMAs tested for IDT strength (GGSP and LVSP Mixtures)

HMA Type	Layer:	Leveling/Top					
	Region:	<i>North, Grand, Bay, Southwest and University Regions (NGBSU)</i>		<i>Metro</i>		<i>Superior</i>	
	Mix Type	Binder PG	HMA#	Binder PG	HMA#	Binder PG	HMA#
M	GGSP	70-28P	49	70-22P	125	-	-
HS	GGSP	76-28P	50	76-22P	126		
M	LVSP	58-28	51	58-22	127	58-34	87
HS	LVSP	64-28	52	64-22	128	64-34P	88
Note: M=Mainline, HS=High Stress							

Table 3 HMAs tested for IDT strength (SUPERPAVE) – Mixtures that do not follow MDOT specifications but are permitted to be used

HMA Type	Mix No:	2		3		4		5	
	Layer:	Base		Base		Leveling/Top		Top	
	Mix Type	Binder PG	HMA#	Binder PG	HMA#	Binder PG	HMA#	Binder PG	HMA#
M	E10			58-28	200				
HS	E10							64-22	202
HS	E30					70-22P	203	70-22P	204
M	E3	58-28	205						
M	E1							64-22	206
M	E1							64-22	207

Note: M=Mainline, HS=High Stress

Table 4 HMAs tested for IDT strength (GGSP and LVSP Mixtures) - Mixtures that do not follow MDOT specifications but are permitted to be used

HMA Type:	Layer:	Leveling/Top					
	Region:	NGBSU		Metro		Superior	
	Mix Type	Binder	HMA#	Binder	HMA#	Binder	HMA#
M	ASCRL	64-28	201				

Note: M=Mainline

3.3 Specimen Preparation

All specimens were compacted according to AASHTO PP60, “Preparation of Cylindrical Performance Test Specimens Using the Superpave Gyratory Compactor (SGC)”, to an air void value of $7 \pm .5\%$, as determined according to the AASHTO T 166-11 “Bulk Specific Gravity of Compacted Hot Mix Asphalt (HMA) Using Saturated Surface-Dry Specimens.” For each unique mixture 3 replicates were generally prepared. A limited number of mixtures had more or less than 3 replicates due to limits in amount of loose mixture available and variability when reaching the target air void content. Each specimen was wet sawed to dimensions of approximately 150 mm diameter and 38 mm height and checked for correct air void content. A

total of 204 specimens were tested with the IDT strength test method for this study. Exact specimens dimensions, air void contents, and number of replicates for each mixture are listed in Appendix A.

3.4 Indirect Strength Testing Procedures

Each specimen was tested for IDT strength in accordance with AASHTO T-322. Due to testing recommendations described in NCHRP 530 and equipment constraints, a few important changes were made in this study and they are listed in the subsequent sections.

3.4.1 Testing Temperature

IDT testing in this study was conducted at -10°C , which is the test temperature required for IDT strength input into Pavement ME Design but differs from AASHTO T-322 requirements. Testing temperature in AASHTO T-322 is recommended based on low temperature PG, PGXX-28 and PG XX-22 are recommended at -10°C while PG XX-16 and stiffer binders are recommended at 0°C . In Pavement ME Design the -10°C testing temperature was selected to represent the undamaged tensile strength of an asphalt mixture in Pavement ME Design as testing in SHRP A-005 showed that peak strength always occurred at temperatures lower than -10°C [6]. Thus testing at -10°C may be considered an accurate and conservative measure of a mixture's "undamaged" tensile strength. The term "undamaged" herein corresponds to the newly constructed asphalt mixture (i.e. no aging or damaged has yet occurred).

3.4.2 Use of LVDTs

As per recommendations put forth in NCHRP 530 and discussed previously, LVDTs were not used in this study. The corrected, or LVDT instrumented, strength of each specimen

was determined using Equation 2, an empirical relationship found to estimate reasonably well corrected strength using uncorrected (uninstrumented) strength [10].

3.4.3 Environmental Chamber

The final modification, actually a limitation, is that specimens were tested in an IDT Test System without an environmental chamber. Due to the IDT Test System chamber inability to maintain a stable test temperature specimens were conditioned and held in an external chamber placed immediately next to the IDT Test System (Figure 7). At the time of testing, each specimen was immediately transferred from the external environmental chamber to the IDT Test System loading frame and loaded to failure in less than 60 seconds from leaving the external environmental chamber. In order to minimize temperature loss during the 60 second transfer process, a dummy specimen with an internal thermocouple was transferred from the external chamber to the testing area. It was observed that the dummy specimen did not lose more than 1°C during this process.



Figure 7 IDT test system consisting of an axial loading device with external environmental chamber

4. RESULTS OF LABORATORY INDIRECT TENSILE TESTING

4.1 Indirect Tensile Strength of Michigan Mixtures

An overview of the average laboratory measured IDT strength for the 62 MDOT asphalt mixtures tested at -10°C as a part of this study is shown in Table 5.

Table 5 Summary of IDT strength values for the State of Michigan asphalt mixtures

Mix No:	3				4				5			
Layer:	Base				Leveling/Top				Top			
Traffic	HMA #	IDT Strength, -10°C			HMA #	IDT Strength, -10°C			HMA#	IDT Strength, -10°C		
		Strength (psi)	SD (psi)	CV (%)		Strength (psi)	SD (psi)	CV (%)		Strength (psi)	SD (psi)	CV (%)
E30	2A	477	22	5	4	483	18	4				
E30	2B	362	21	6								
E10	18A	343	49	14	20A	452	32	7	20B	448	19	4
E10	18B	463	30	7	20C	395	23	6	21	454	19	4
E10	200				23	462	15	3	24A	372	27	7
E10									24B	498	16	3
E3	26A	400	19	5	28A	483	15	3	29A	399	12	3
E3	26B	338	29	9	28B	416	20	5	29B	426	22	5
E3	26C	346	12	3	31A	442	36	8	32A	460	19	4
E3	62	413	19	5	31B	470	11	2	32B	453	8	2
E3					64	388	45	12	65	362	10	3
E3					67	402	20	5				
E1					44	405	27	7	45	346	34	10
E1					47	433	4	1	48	422	21	5
E03									37	455	20	4

Table 5 (cont'd)

Mix No:	Miscellaneous				Mix No:	4				5			
Layer:	Miscellaneous				Layer:	Leveling/Top				Top			
Mix	HMA #	IDT Strength, -10°C			Traffic	HMA #	IDT Strength, -10°C			HMA#	IDT Strength, -10°C		
		Strength (psi)	SD (psi)	CV (%)			Strength (psi)	SD (psi)	CV (%)		Strength (psi)	SD (psi)	CV (%)
GGSP	49A	387	14	4	E50					97	508	5	1
GGSP	49C	336	16	5	E30	90A	455	0	0	204	560	12	2
LVSP	51A	347	40	12	E30	203	451	13	3				
LVSP	51B	405	14	4	E10	102	487	17	4	103	427	70	16
LVSP	51C	379	12	3	E10	105	449	32	7	202	512	8	2
LVSP	127	389	40	10	E10					209A	453	9	2
ASCRL	201	276	7	3	E10					209B	419	31	7
2E3	205	321	37	12	E3	67	402	20	5	68	410	24	6
LVSP	208	425	18	4	E3	108	467	15	3	109	480	28	6
					E3	111	512	10	2	112	533	9	2
					E1	80	409	15	4	81	357	0	0
					E1	85	403	11	3	86	417	16	4
					E1					206	468	22	5

The average IDT strength of all mixtures was 426 psi. The lowest recorded IDT strength was 276 psi, measured from mix 201 an Asphalt Stabilized Crack Relief Layer (ASCRL) mixture. The highest IDT strength recorded was 560 psi, measured from mix 204 a MDOT designated 5E30 High Stress mixture.

Major state and highway mixtures used in the State of Michigan are designated using a two part nomenclature system. The first part of the designation details the location in the pavement system in which the mix will be used (base, leveling, leveling/top, or top course). The second part of the designation is termed the mix type and details the expected design traffic value in millions of ESALs. For instance a mix designated 5E30 would be used as a top course and is designed to withstand 30 million ESALs. The IDT strength values for each of the ESAL design categories was examined to investigate the use of the MDOT mixture classification systems ability to be used as a thermal cracking resistance parameter during design. In Table 5 mixtures with greater IDT strength are generally designated as Mix No. 4 and 5 while mixtures with the lower IDT strength are generally designated as Mix No. 2 and 3, GGSP, and LVSP.

4.2 Fracture Work of Michigan Mixtures

It is recalled that fracture work of a mixture is defined as the area under the load versus vertical deformation curve and can be reported as total fracture work (Figure 6), which consists of pre-peak work (fracture work measured until failure), and post-peak fracture work (fracture work measured after failure). Measured total, pre, and post fracture work for the mixtures tested in this study are given in Table 6.

Table 6 Summary of total work values for the State of Michigan asphalt mixtures

Layer:	Base				Leveling/Top					Top		
Traffic	HMA #	Total Work, -10°C			HMA #	Total Work, -10°C			HMA#	Total Work, -10°C		
		Total Work (lb*in.)	SD (lb*in.)	CV (%)		Total Work (lb*in.)	SD (lb*in.)	CV (%)		Total Work (lb*in.)	SD (lb*in.)	CV (%)
E30	2A	280	75	27	4	415	53	13				
E30	2B	419	92	22								
E10	18A	365	164	45	20A	269	61	23	20B	341	24	7
E10	18B	273	87	32	20C	362	86	24	21	281	42	15
E10	200	242	11	5	23	446	63	14	24A	527	68	13
E10									24B	459	84	18
E3	26A	412	0	0	28A	225	45	20	29A	280	11	4
E3	26B	430	11	3	28B	185	33	18	29B	202	23	12
E3	26C	349	63	18	31A	281	72	26	32A	327	42	13
E3	62	508	97	19	31B	283	32	11	32B	406	79	20
E3					64	246	77	31	65	324	40	12
E3					67	522	85	16				
E1					44	226	45	20	45	323	40	12
E1					47	245	42	17	48	213	48	22
E03									37	515	154	30

Table 6 (cont'd)

Mix No:	Miscellaneous				Mix No:	4				5			
Layer:	Miscellaneous				Layer:	Leveling/Top				Top			
Mix	HMA #	Total Work, -10°C			Traffic	HMA #	Total Work, -10°C			HMA#	Total Work, -10°C		
		Total Work (lb*in.)	SD (lb*in.)	CV (%)			Total Work (lb*in.)	SD (lb*in.)	CV (%)		Total Work (lb*in.)	SD (lb*in.)	CV (%)
GGSP	49A	499	141	28	E50					97	258	28	11
GGSP	49C	1014	258	25	E30	90A	182	0	0	204	383	70	18
LVSP	51A	544	130	24	E30	203	337	60	18				
LVSP	51B	215	47	22	E10	102	343	81	23	103	333	212	64
LVSP	51C	294	27	9	E10	105	312	58	19	202	185	21	11
LVSP	127	307	98	32	E10					209A	200	41	20
ASCRL	201	232	83	36	E10					209B	196	52	27
LVSP	208	174	22	13	E3	67	522	85	16	68	405	40	10
					E3	108	302	65	22	109	241	46	19
					E3	111	338	9	3	112	238	20	8
					E1	80	514	96	19	81	193	0	0
					E1	85	622	147	24	86	538	116	22
					E1					206	178	20	11

Table 7 Summary of pre fracture work values for the State of Michigan asphalt mixtures

Mix No:	3				4				5			
Layer:	Base				Leveling/Top				Top			
Traffic	HMA #	Pre Work, -10°C			HMA #	Pre Work, -10°C			HMA#	Pre Work, -10°C		
		Pre Work (lb*in.)	SD (lb*in.)	CV (%)		Pre Work (lb*in.)	SD (lb*in.)	CV (%)		Pre Work (lb*in.)	SD (lb*in.)	CV (%)
E30	2A	275	68	25	4	300	30	10				
E30	2B	261	29	11								
E10	18A	228	36	16	20A	264	53	20	20B	263	37	14
E10	18B	244	47	19	20C	247	33	14	21	281	42	15
E10	200	242	11	5	23	320	4	1	24A	287	17	6
E10									24B	335	17	5
E3	26A	247	0	0	28A	225	45	20	29A	260	24	9
E3	26B	220	17	8	28B	183	29	16	29B	198	20	10
E3	26C	247	23	9	31A	254	38	15	32A	291	20	7
E3	62	265	36	14	31B	279	28	10	32B	275	37	13
E3					64	202	42	21	65	274	8	3
E3					67	253	35	14				
E1					44	226	45	20	45	252	2	1
E1					47	245	42	17	48	213	48	22
E03									37	254	56	22

Table 7 (cont'd)

Mix No:	Miscellaneous				Mix No:	4				5			
Layer:	Miscellaneous				Layer:	Leveling/Top				Top			
Mix	HMA #	Pre Work, -10°C			Traffic	HMA #	Pre Work, -10°C			HMA#	Pre Work, -10°C		
		Pre Work (lb*in.)	SD (lb*in.)	CV (%)			Pre Work (lb*in.)	SD (lb*in.)	CV (%)		Pre Work (lb*in.)	SD (lb*in.)	CV (%)
GGSP	49A	260	13	5	E50					97	258	28	11
GGSP	49C	200	24	12	E30	90A	182	0	0	204	377	60	16
LVSP	51A	226	29	13	E30	203	289	60	21				
LVSP	51B	215	47	22	E10	102	297	28	9	103	218	41	19
LVSP	51C	236	24	10	E10	105	297	35	12	202	185	21	11
LVSP	127	243	37	15	E10					209A	200	41	20
ASCRL	201	180	20	11	E10					209B	192	47	24
LVSP	208	174	22	13	E3	67	253	35	14	68	292	26	9
					E3	108	298	58	19	109	241	46	19
					E3	111	321	19	6	112	238	20	8
					E1	80	294	32	11	81	193	0	0
					E1	85	254	31	12	86	287	33	12
					E1					206	178	20	11

Table 8 Summary of post fracture work values for the State of Michigan asphalt mixtures

Mix No:	3				4				5			
Layer:	Base				Leveling/Top				Top			
Traffic	HMA #	Post Work, -10°C			HMA #	Post Work, -10°C			HMA#	Post Work, -10°C		
		Post Work (lb*in.)	SD (lb*in.)	CV (%)		Post Work (lb*in.)	SD (lb*in.)	CV (%)		Post Work (lb*in.)	SD (lb*in.)	CV (%)
E30	2A	5	9	173	4	115	32	28				
E30	2B	158	77	49								
E10	18A	137	144	105	20A	5	8	173	20B	78	27	35
E10	18B	30	46	155	20C	115	96	83	21	0	0	0
E10	200	0	0	0	23	125	61	49	24A	240	78	32
E10									24B	123	90	73
E3	26A	165	0	0	28A	0	0	0	29A	20	35	173
E3	26B	210	8	4	28B	2	5	200	29B	4	5	122
E3	26C	102	49	48	31A	27	37	136	32A	35	41	116
E3	62	243	130	54	31B	4	7	173	32B	131	43	32
E3					64	43	50	116	65	50	49	98
E3					67	269	108	40				
E1					44	0	0	0	45	71	41	58
E1					47	0	0	0	48	0	0	0
E03									37	261	210	80

Table 8 (cont'd)

Mix No:	Miscellaneous				Mix No:	4				5			
Layer:	Miscellaneous				Layer:	Leveling/Top				Top			
Mix	HMA #	Post Work, -10°C			Traffic	HMA #	Post Work, -10°C			HMA#	Post Work, -10°C		
		Post Work (lb*in.)	SD (lb*in.)	CV (%)			Post Work (lb*in.)	SD (lb*in.)	CV (%)		Post Work (lb*in.)	SD (lb*in.)	CV (%)
GGSP	49A	239	144	60	E50					97	0	0	0
GGSP	49C	813	247	30	E30	90A	0	0	0	204	6	11	173
LVSP	51A	318	157	49	E30	203	49	49	101				
LVSP	51B	0	0	0	E10	102	46	53	116	103	115	193	168
LVSP	51C	59	14	25	E10	105	15	31	200	202	0	0	0
LVSP	127	64	67	106	E10					209A	0	0	0
ASCRL	201	52	63	123	E10					209B	4	7	173
LVSP	208	0	0	0	E3	67	269	108	40	68	112	48	43
					E3	108	4	7	200	109	0	0	0
					E3	111	16	28	173	112	0	0	0
					E1	80	221	123	56	81	0	0	0
					E1	85	367	178	48	86	251	148	59
					E1					206	0	0	0

The average total fracture work of all mixtures was 340 lb*in. The lowest total fracture work was 174 lb*in., measured from mix 208 a Low Volume Superpave (LVSP) mixture. The highest total fracture work recorded was 1014 lb*in., measured from mix 49C a Gap Graded Superpave (GGSP) mixture.

A comparison of the pre and post fracture work for all 62 mixtures tested in this study is depicted in Table 7 and Table 8. The average pre fracture work was 250 lb*in and the average post fracture work was 91 lb*in. The greatest pre fracture work was 377 lb*in., measured from mix 204 (5E30 High Stress). The lowest pre fracture work recorded was 174 lb*in, measured from mix 208 (LVSP). The highest post fracture work recorded was 813 lb*in., measured from mix 49C (GGSP). The lowest post fracture work recorded was 0 lb*in. Post fracture work of a mixture was generally less than pre fracture work and 16 of the 62 mixtures tested in this study had no measured post fracture work.

The relationship between total fracture work and IDT strength is shown in Figure 8. While there is high scatter in the data, a general trend exists as IDT strength increases total fracture work decreases. This trend is reasonable as softer mixes can generally be expected to exhibit greater fracture work and lower IDT strength, while stiffer mixes have greater IDT strength and lower fracture work.

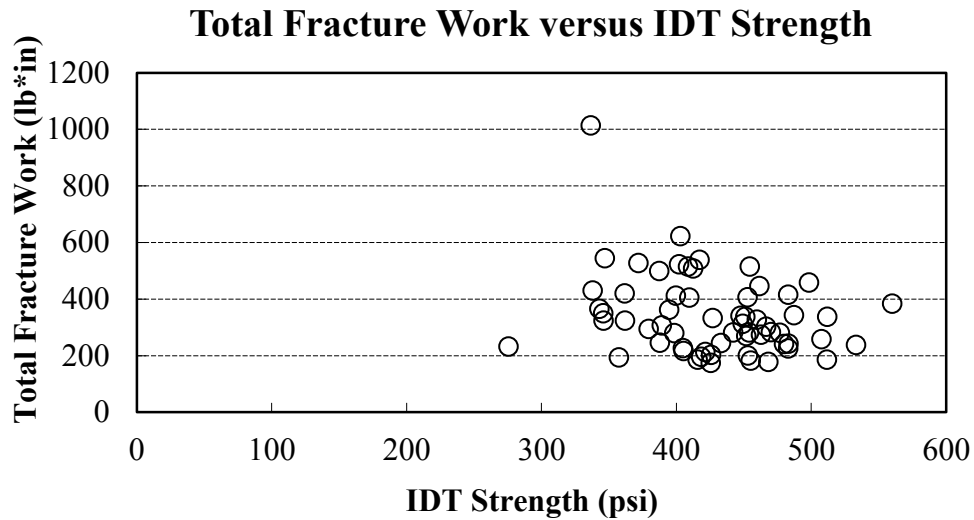


Figure 8 Total fracture work versus IDT strength relationship

4.3 MDOT Mix Designation and IDT Strength

The IDT strength values for each of the ESAL design categories was examined to investigate the use of the MDOT mixture classification systems ability to be used as a thermal cracking resistance parameter during design. Figure 9 shows the relationship between ESAL and IDT strengths of the asphalt mixtures tested. As shown, the IDT strength generally increases with the design ESAL of the mixtures. However a clear relationship is not visible. Some of the mixtures designated with ESAL of 1 million have higher IDT strength than mixtures designated with ESALs of 10, 30, and 50 million. This is meaningful because besides ESAL, there are many other factors affecting the IDT strength. A clear trend should not be anticipated since there are many variables (e.g., aggregate gradation, PG, VMA, VFA...etc.) that play a role in IDT strength.

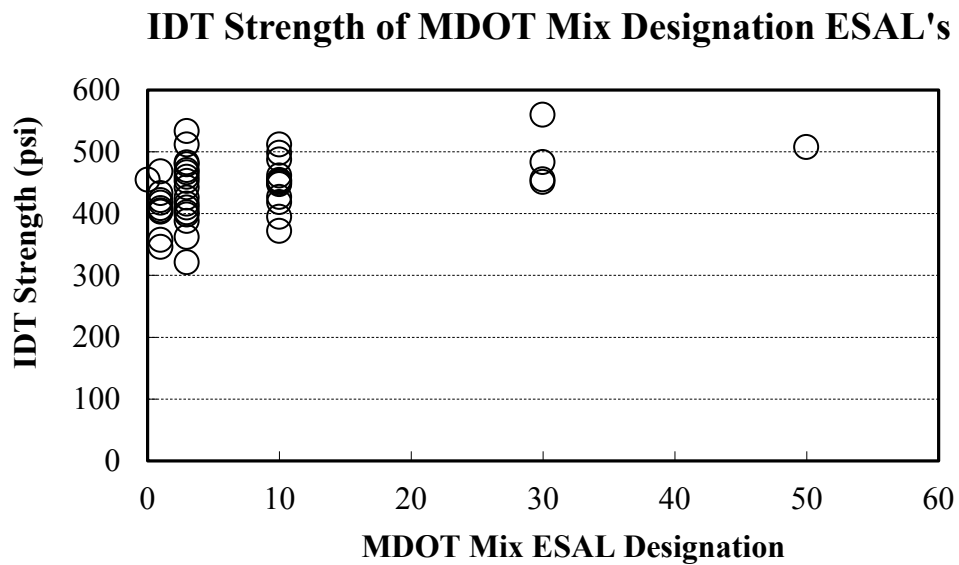


Figure 9 Laboratory measured IDT strength for MDOT Mix ESAL designation categories for leveling and top course pavement layers

Figure 10 shows the relationship between MDOT Mix ESAL designation and total fracture work. As shown, even though there is significant scatter in the data, a general decrease in fracture work is observed with increasing ESAL. As was seen with mixture IDT strength a clear trend should not be anticipated since there are many variables (e.g., aggregate gradation, PG, volumetrics) that affect a mixture's fracture work.

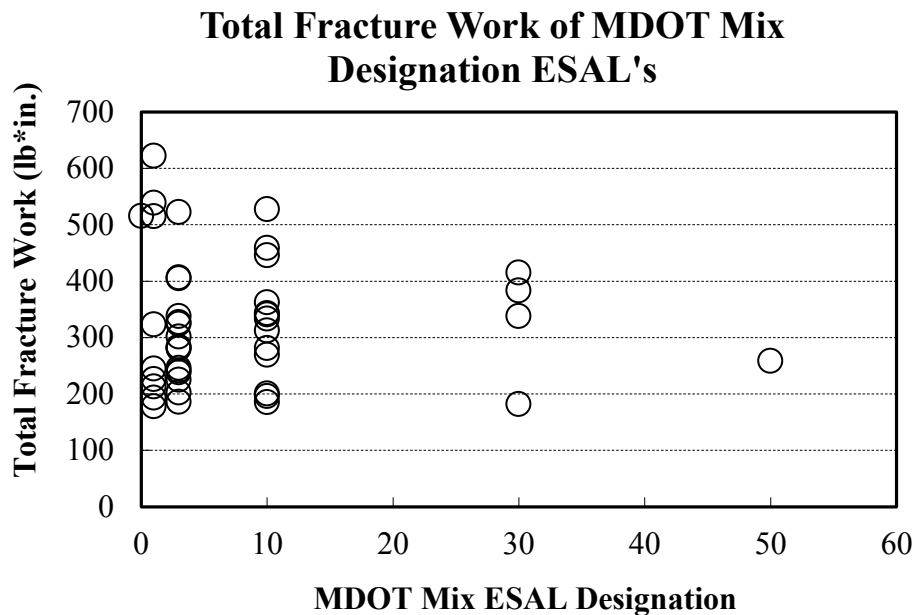


Figure 10 Laboratory measured total fracture work for MDOT Mix ESAL designation categories for leveling and top course pavement layers

4.4 Superpave PG and IDT Strength

Superpave performance grading (PG) is a binder characterization system developed to relate binder performance to the climatic conditions in which it will be utilized. For the PG grading process, binder undergoes a battery of tests including Rolling Thin Film Oven (RTFO), Pressure Aging Vessel (PAV), Rotational Viscometer (RV), Dynamic Shear Rheometer (DSR), Bending Beam Rheometer (BBR), and Direct Tension Tester (DDT). Based on the results of these tests, a PG is determined consisting of a high grade; the average seven-day maximum pavement temperature (°C), and a low grade; the minimum expected pavement temperature (°C) likely to be experienced. For instance, in the northern US, a binder graded PG 58-40 would be expected to outperform a PG 58-16 binder in regards to thermal cracking due to its greater low

PG classification. The IDT strength of the Michigan mixtures used in this study are depicted as a function their low PG (-22, -28, or -34) and their high PG (58, 64, or 70) in Figure 11 and Figure 12, respectively.

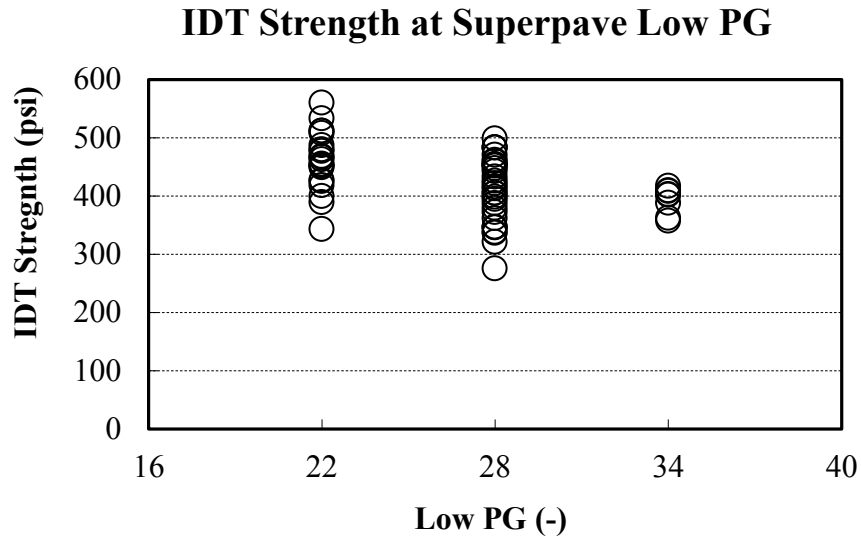


Figure 11 IDT strength versus Low Temperature PG relationship

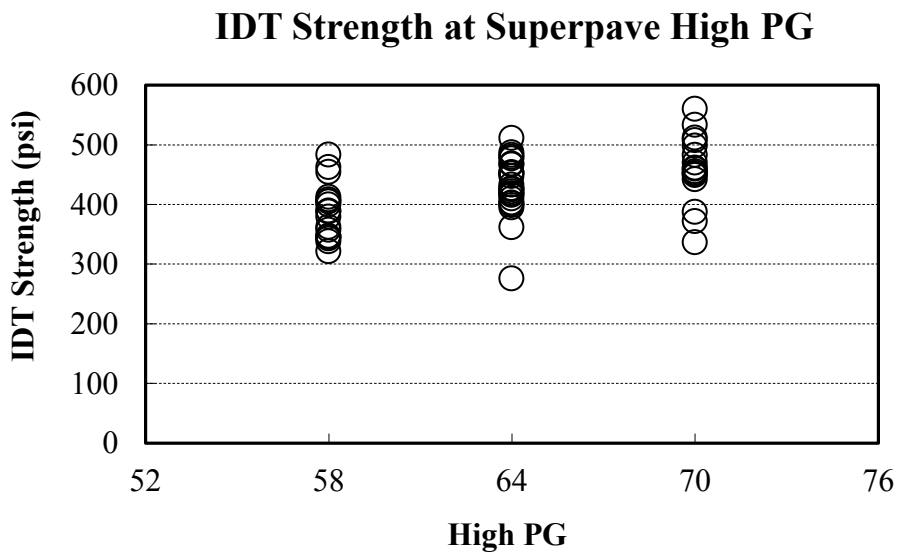


Figure 12 IDT strength for high PG characterization of Michigan asphalt mixtures

As shown, while there is scatter in the data, IDT strength generally decreases with an increase in low PG. This is somewhat meaningful since as low PG increases, the binder becomes softer (and less brittle). Soft binder perhaps leads to low IDT strength. Figure 12 shows the relationship between the high PG and IDT strength, where an increase in IDT strength is observed with increasing high PG. This is consistent with the trend with low PG where stiffer binder (higher the high PG) results in higher IDT strength.

The relationship between total fracture work and low and high PG is shown in Figure 13 and Figure 14, respectively. As low PG increases total fracture work generally increases, although there is significant scatter in the data. This is somewhat expected as at a greater low PG the softer binder (less brittle) should exhibit greater fracture work. There is no clear relationship between high PG and total fracture work, as little difference is seen in total fracture work for different high PG (Figure 14).

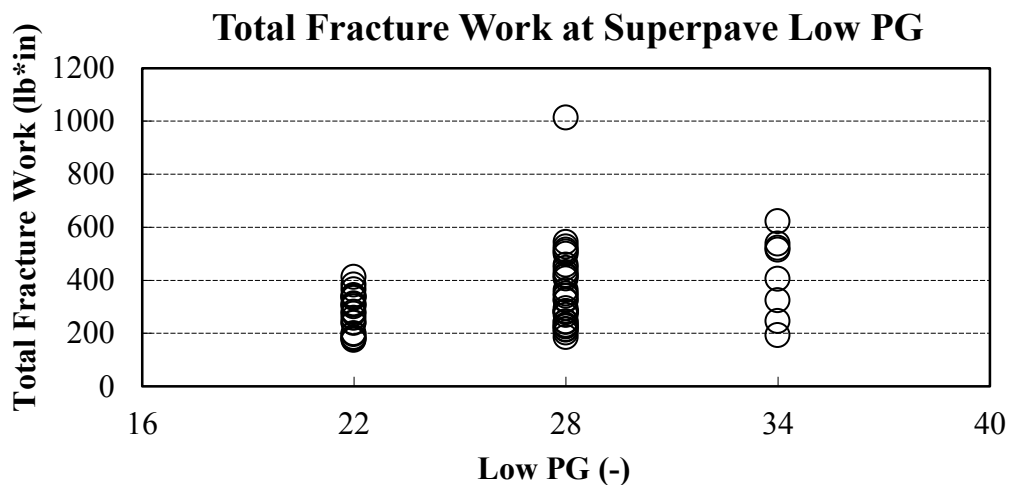


Figure 13 Fracture work for low temperature Superpave PG characterization of Michigan asphalt mixtures

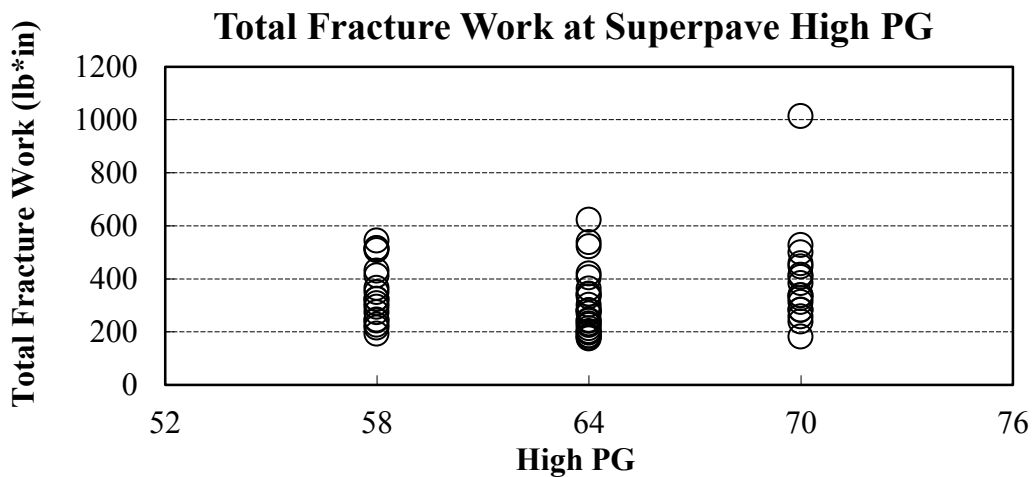


Figure 14 Fracture work for high temperature Superpave PG characterization of Michigan asphalt mixtures

This is evidence of two important characteristics of low temperature performance characterization of asphalt mixtures. Firstly, although the Superpave PG system is an improvement upon binder classification methods binders can still have significantly different performance characteristics within a PG designation. Secondly IDT strength of an asphalt mixture is not a function of solely the type of binder used in mixture design. IDT strength cannot be evaluated based on PG or MDOT mix designation alone. Other mixture components such as aggregate source and gradation, volumetric, and mixture properties must be considered when examining the IDT strength of an asphalt mixture. Pavement engineers should use caution when anticipating increased IDT strength as a result of increasing the low temperature PG magnitude and should instead utilize laboratory testing or IDT strength prediction models to examine the effect of mixture design on thermal cracking resistance.

4.5 Warm Mix Asphalt IDT Properties

A number of warm mix asphalt (WMA) mixtures were characterized with the IDT strength test in this study. A comparison of their IDT strength and total fracture work is shown in Figure 15 and Figure 16. Comparison of WMA and HMA mixtures was made between mixtures having similar PG, percent binder, and gradations, i.e. mixture 2A (HMA) was compared with mixture 2B (WMA) and mixture 209A (HMA) was compared to mixture 209B (WMA)(Appendix A). Mixture 208 (WMA) was not examined in this analysis, as it did not have a comparable HMA mixture.

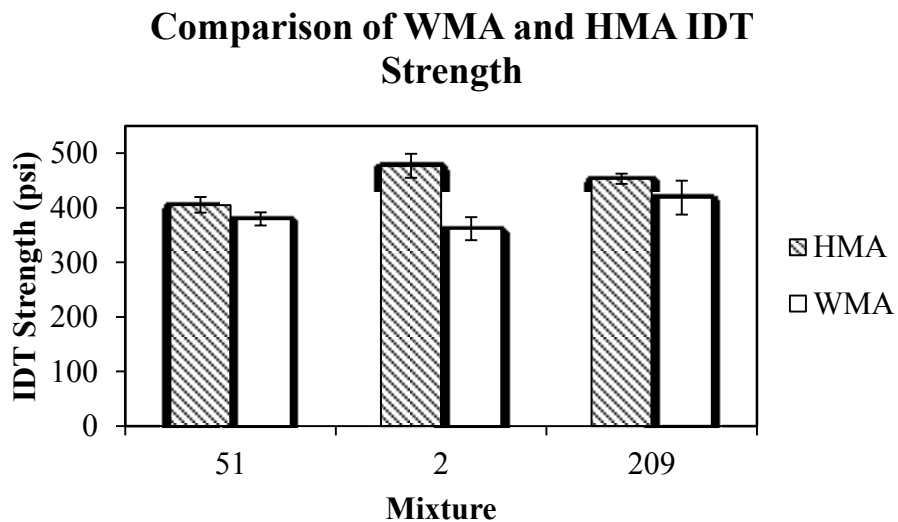


Figure 15 IDT strength for comparable WMA and HMA mixtures

As shown in Figure 15, the WMA mixtures had lower IDT strength values as compared to their similar HMA mixtures. Figure 16 shows a comparison of total fracture work for the similar WMA and HMA mixtures. Generally it is shown that WMA mixtures tested in this study have higher total fracture work as compared to their similar HMA mixtures.

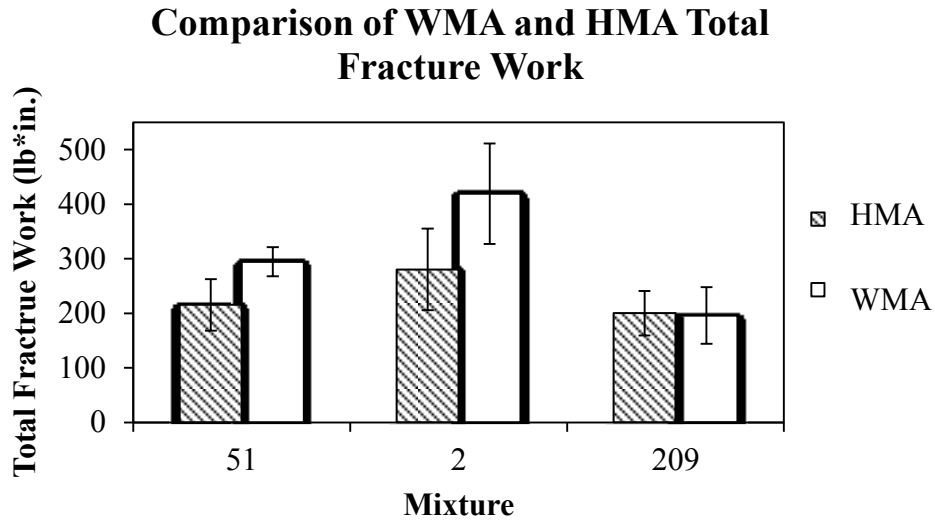


Figure 16 IDT fracture work for comparable WMA and HMA mixtures

A comparison of post fracture work for WMA and HMA mixtures is shown in Figure 17. It is shown that all WMA mixtures have a greater post fracture work as compared to their similar HMA mixtures. It is noted that all HMA mixtures were shown to have zero or nominal post fracture work, a property that correlates to crack growth and propagation. When compared to tested HMA mixtures similar WMA mixtures tested in this study may be thought to exhibit slower rates of thermal cracking growth.

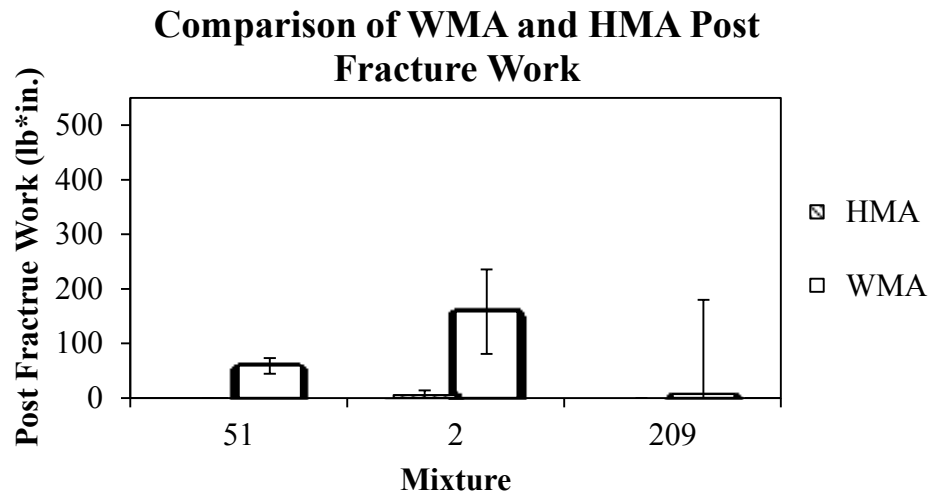


Figure 17 IDT post fracture work for comparable WMA and HMA mixtures

5. INDIRECT TENSILE STRENGTH PREDICTION MODELS

5.1 Introduction to Indirect Tensile Strength Prediction for Pavement ME Design

In Pavement ME Design thermal cracking distress prediction directly depends on accurate material characterization, i.e. IDT strength at -10°C and creep compliance. Over prediction of IDT strength in Level 3 analysis of the Pavement ME Design can lead to higher thermal cracking rates while under prediction can lead to over designed pavements, both costly to state transportation agencies. Figure 18 depicts a preliminary sensitivity analysis of IDT strength input on thermal cracking prediction in Pavement ME Design. For a scenario of a 4” flexible pavement lift (PG 58-22) constructed in Detroit, MI the amount of thermal cracking was determined as a function of different IDT strength values. An IDT strength of 100 psi was used as it is the lower boundary limit of IDT strength input into Pavement ME Design while an IDT strength of 500 psi was used as it was generally a typical upper limit of IDT strength of the mixtures tested in this study. In Figure 18 it is shown that the amount of thermal cracking varies with IDT strength and thermal cracking prediction is dependent on the IDT strength value input into Pavement ME Design software. To successfully predict thermal cracking in Pavement ME Design it is necessary to accurately determine material inputs such as IDT strength. If testing is not possible or feasible, an accurate predictive equation for IDT strength is necessary to improve the predictions of Pavement ME Design.

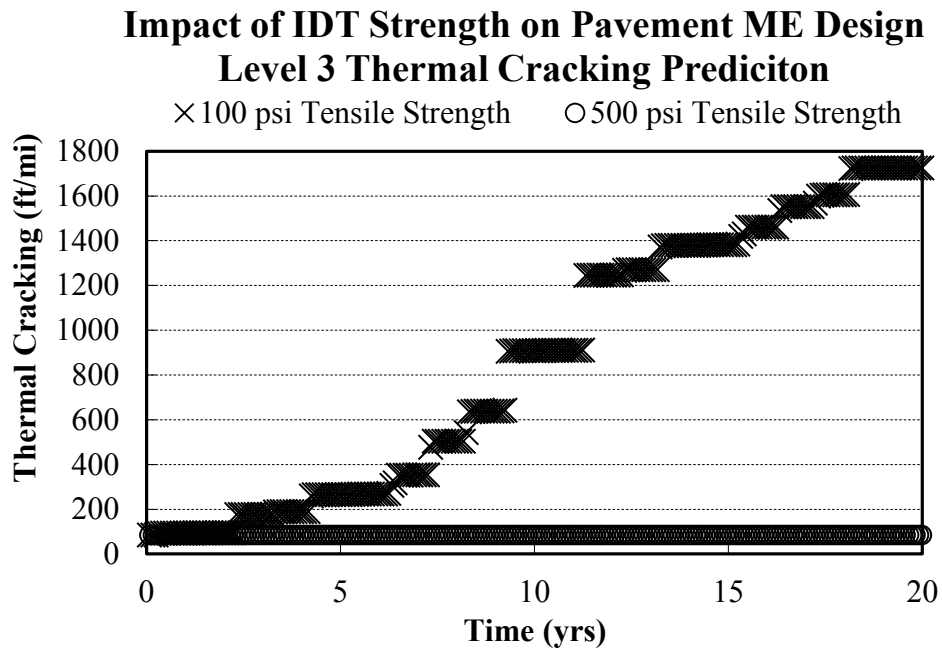


Figure 18 Effect of IDT strength input in Pavement ME Design Level 3 thermal cracking analysis for a 4", PG 58-22 flexible pavement constructed in Detroit, Michigan.

In this study three models were developed to improve IDT strength prediction for Michigan mixtures; (i) a locally calibrated Pavement ME Design IDT strength model, (ii) a newly developed linear IDT strength model, and (iii) an artificial neural network (ANN) based model. The development of each IDT model is explained and then evaluated for prediction performance with respect to current Pavement ME Design IDT strength prediction. Increased IDT strength prediction performance has the potential to firstly increase Level 3 thermal cracking prediction accuracy with the use of more accurate material inputs. Secondly calibration or development of a model with adequate prediction performance could be utilized to predict IDT strength for Level 1 and 2 Pavement ME Design analyses, which are currently measured by laboratory testing. Lastly development of a model that utilizes inputs readily obtainable by

pavement designers and does not require costly and time consuming laboratory testing would be advantageous to state agencies.

5.2 Model Evaluation

The performance of a Michigan calibrated Pavement ME Design IDT strength model and a newly developed IDT linear regression model were evaluated using goodness-of-fit statistics, visual inspection with respect to the line of equality (LOE), and local bias statistics. Goodness-of-fit statistics include S_e/S_y and R^2 and are calculated as follows.

$$S_e = \sqrt{\frac{\sum(y-\hat{y})^2}{(n-k)}} \quad (6)$$

$$S_y = \sqrt{\frac{\sum(y-\bar{y})^2}{(n-1)}} \quad (7)$$

$$R^2 = 1 - \frac{(n-k)}{(n-1)} \left(\frac{S_e}{S_y}\right)^2 \quad (8)$$

Where:

S_e = Standard error of estimate,

S_y = Standard deviation,

R^2 = Correlation coefficient,

y = Measured IDT strength,

\hat{y} = Predicted IDT strength,

\bar{y} = Mean value of measured IDT strength,

n = Sample size

k = Number of independent variables in the model

S_e/S_y is a measure of prediction improvement over the empirical model, a smaller S_e/S_y ratio is indicative of improved prediction by the model. The R^2 is a measure of model accuracy, a value closer to 1 indicates better estimation by the model [31]. Evaluation by visual inspection is accomplished by examining the plotted measured versus predicted values with respect to the LOE. If the plotted values are fairly equally distributed around the LOE then the empirical model will generally exhibit good correlation to the measured data [30]. Slope and intercept are a measure of local bias in the empirical models and were calculated by fitting an unconstrained line of best fit to the measured versus predicted data in Microsoft Excel. Local bias statistics can indicate patterns of over prediction or under prediction by the empirical model that may not be discerned by either goodness-of-fit statistics or visual inspection [30].

5.3 Local Calibration of Pavement ME Design Strength Prediction Model

The first effort to improve Pavement ME Design IDT strength prediction performance was local calibration of the original IDT equation developed by Witczak et al [6] (Equation 5) for calculation of IDT strength in the TC Model. 36 of the 62 MDOT mixtures tested in this study were used in the local calibration process since only 36 of the binders were available for Penetration testing. It is noted that Penetration testing is an input to the Pavement ME IDT strength predictive model. Also, only these 36 mixtures had available binder characterization data, $ARTFO$ and VTS , a required input into the Pavement ME Design IDT strength predictive

model. Air void and Penetration Grade values for the 36 mixtures used in the local calibration are listed in Table 9. ARTFO and VTS binder properties, measured as part of a larger material characterization project at Michigan State University, are listed in Table 9.

Table 9 Binder and Mixture Properties of 36 MDOT Mixtures used in Michigan Calibration of the Pavement ME Design Strength Prediction Model Developed by Witczak

Sample ID	Pen₇₇ Average (0.1 mm)	ARTFO	VFA (%)	V_a (+-.5) (%)
2A	55.3	9.550	71.98	7.00
4	61.7	7.519	70.01	7.00
18B	42.3	9.935	70.51	7.00
20B	55.0	8.201	68.66	7.00
21	68.7	8.604	68.30	7.00
26A	63.0	10.265	68.40	7.00
26B	74.7	9.697	68.56	7.00
28B	49.3	9.926	69.32	7.00
29B	69.7	10.207	68.31	7.00
31A	74.3	7.783	68.62	7.00
31B	52.0	8.146	68.91	7.00
32A	49.7	7.819	67.36	7.00
37	67.3	9.817	68.60	7.00
44	66.7	8.494	69.82	7.00
45	111.3	11.701	68.27	7.00
47	63.0	8.170	69.86	7.00
48	51.3	9.066	68.30	7.00
49A	77.3	7.553	69.37	7.00
62	67.0	10.039	72.39	7.00
65	141.0	10.220	67.98	7.00
67	103.3	7.540	71.82	7.00
68	80.3	7.795	70.35	7.00
86	129.7	7.611	68.44	7.00
102	49.7	9.540	70.49	7.00
103	56.0	9.978	70.03	7.00
108	50.7	9.709	70.58	7.00
109	58.0	9.605	70.59	7.00
111	55.0	7.616	70.10	7.00
112	40.3	7.904	69.47	7.00
127	53.3	10.162	69.63	7.00
200	58.0	8.720	69.89	7.00
202	33.3	9.903	67.96	7.00

Table 9 (cont'd)

Sample ID	Pen77 Average (0.1 mm)	ARTFO	VFA (%)	V _a (+-.5) (%)
204	33.3	8.017	68.49	7.00
205	71.0	10.119	70.85	7.00
206	36.7	9.388	71.14	7.00

For local calibration coefficients of the original Pavement ME Design IDT strength model (Equation 5) were varied using Microsoft Excel Solver package to reduce the sum of the squares between measured and Pavement ME Design predicted IDT strengths. Coefficient labeling of the original Pavement ME Design IDT strength model is shown in Equation 9.

$$S_t = C1 + (C2)V_a + (C3)V_a^2 + (C4)VFA + (C5)VFA^2 + (C6)\log(Pen77) + (C7)\log(ARTFO) \quad (9)$$

Values of the original Pavement ME Design IDT strength model coefficients before and after Michigan calibration are listed in Table 10.

Table 10 Comparison of the original and Michigan calibrated Pavement ME Design IDT strength Model Calibration Coefficients

Coefficient	IDT Prediction Model	
	Original Pavement ME Design Witczak	Michigan Calibrated Witczak Pavement ME Design
C1	7416.7120	6377.5873
C2	-114.0160	-112.9216
C3	-0.3040	-0.3039
C4	-122.5920	-122.5112
C5	0.7040	0.8589
C6	405.7100	-246.1319
C7	-2039.2960	-346.4313

It is of note that the coefficient assigned to the Pen₇₇ parameter changes both sign and magnitude (Table 10) in local calibration with the Michigan mixes. This is reasonable as softer binders are generally expected to have higher penetration and lower IDT strength. Thus the higher Pen₇₇ in the Michigan calibrated model the lower predicted IDT strength will be. Comparison of the measured versus predicted IDT strength values for the original and Michigan calibrated IDT strength models are plotted in Figure 19 and Figure 20, respectively. Visual inspection of the original Pavement ME Design IDT strength model shows points are poorly distributed with respect to the LOE while after calibration points are fairly well distributed along the LOE.

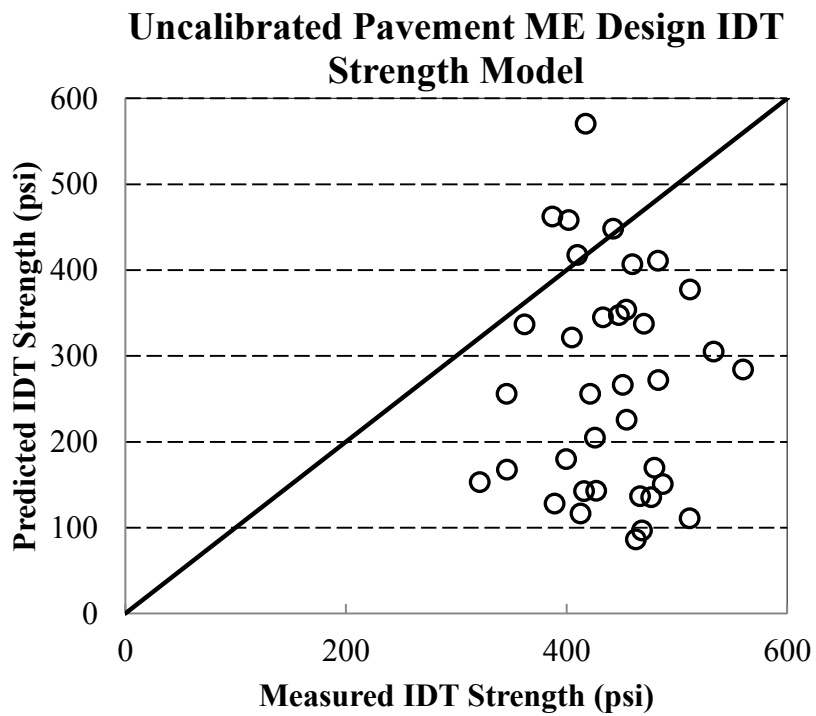


Figure 19 Original Pavement ME Design IDT Strength Model for 36 MDOT mixtures with respect to the LOE

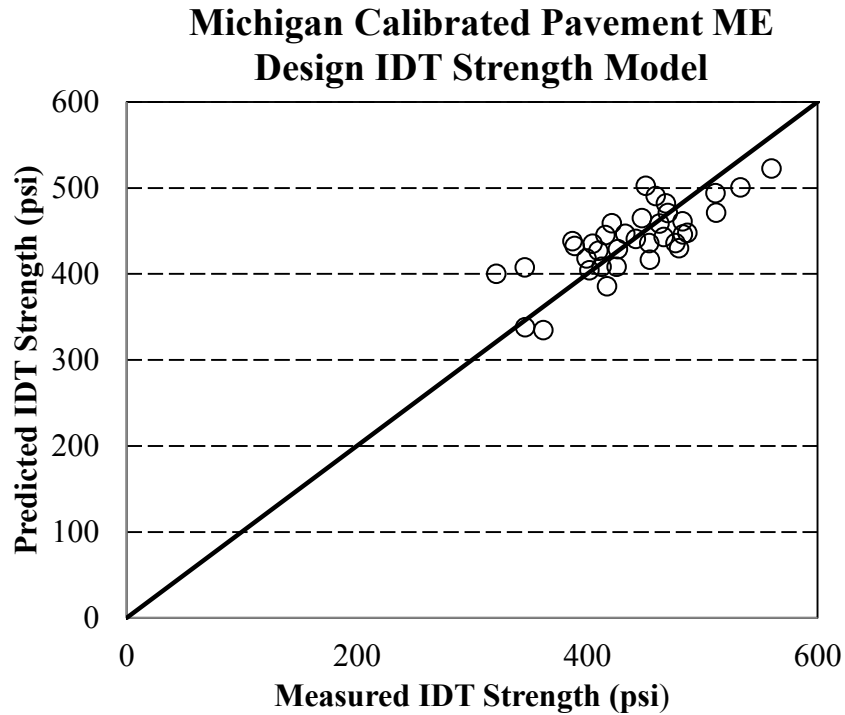


Figure 20 Michigan Calibrated Pavement ME Design IDT Strength Model for 36 MDOT mixtures with respect to the LOE

Table 11 overviews the performance evaluation criteria before and after local calibration. The Michigan calibrated Pavement ME Design model shows increased performance with a lower standard error of estimate/standard deviation, $S_e/S_y = 0.0598$, and higher correlation coefficient, $R^2 = 0.663$, as compared to the original Pavement ME Design model. Local bias statistics, unconstrained slope and intercept, of the Michigan calibrated model are 0.5939 and 178.48, respectively, indicating a tendency of the calibrated model to under predict IDT strength.

Comparison of the original Pavement ME Design model before and after calibration shows substantially increased distribution around the LOE.

Table 11 Comparison of model performance evaluation parameters measured for Original Pavement ME Design and Calibrated IDT strength prediction models for 36 MDOT asphalt mixtures

Model Performance Measure	IDT Prediction Model	
	Original	Calibrated
R^2	0.000	0.598
S_e/S_y	4.436	0.663
Visual Inspection (LOE)	Poorly distributed	Well distributed
Unrestrained Slope	-0.0402	0.5939
Unrestrained Intercept	283.87	178.48

5.4 Linear Strength Prediction Model

The second effort to improve Pavement ME Design IDT strength prediction performance was development of new model using linear regression techniques. IBM[©] SPSS[©] Statistics software (SPSS) was used to perform a statistical analysis on variables with a potential impact on IDT strength. The purpose of the statistical analysis was to firstly determine if there was a relationship between measured IDT strength and mix design properties and volumetrics. Secondly, determine if the relationship is positive or negative. And thirdly determine the strength of the relationship between the two variables. Once the relationship of the mix design and volumetric variables to IDT strength was determined, linear regression was performed with parameters that significantly correlated to IDT strength to develop a linear model. In addition to a possible increase in IDT prediction performance, the advantage of such a model is the ease of

obtaining the input parameters. All inputs are readily obtainable by engineers via a MDOT Job Mix Formulas (JMFs) and do not require costly and often time consuming laboratory testing. A JMF is a document provided to the paving contractor containing detailed mix design information including mixture properties, volumetrics, gradation, compaction and placement temperatures, and other important mix information.

A Pearson correlation analysis was performed using SPSS to determine which JMF variables were significantly correlated to IDT strength. When determining significant relationships, the *p*-value statistic was used. If the *p*-value is less than 0.05 then the correlation coefficient is considered to be significant at the 0.05 level and if the *p*-value is less than 0.01 then the correlation coefficient is considered to be significant at the 0.01 level. JMF parameters having a significance at least 0.05 were used in construction of a linear IDT strength model for this study. Table 12 summarizes the JMF parameters that correlated significantly with laboratory measured IDT strength, their respective *p*-values, and type of relationship (positive or negative).

Table 12 MDOT JMF parameters found to be significantly correlated with measured IDT strength using a Pearson Correlation analysis. Correlation significance, either at the .01 or .05 level, and the relationship of the parameter, either positive (+) or negative (-), is also listed

Correlated JMF Variable	Correlation Significance	Relationship
Polymer Modified	0.01	+
High PG	0.01	+
Low PG	0.01	-
Fines/Asphalt Ratio	0.05	+
Angularity	0.01	+
% Passing 1/2"	0.01	+
% Passing 3/8"	0.01	+
% Passing #4	0.01	-
% Passing #8	0.05	+
% Passing #100	0.05	+
% Passing #200	0.05	-
% Air Voids	---	---

It is of note that laboratory measured IDT strength correlated with not only asphalt binder parameters (Polymer Modification, High and Low PG), but also with aggregate parameters (% Passing 1/2", 3/8", #4, #8, #100, and #200 sieves and the Fines/Asphalt Ratio). This is evidence that aggregate gradation is also a significant factor influencing low temperature IDT strength in addition to asphalt binder properties.

For development of a linear Pavement ME Design IDT strength predictive equation, significantly correlated JMF parameters (Table 12) were assigned coefficients (Equation 10) and then varied using Microsoft Excel Solver package to reduce the sum of the squares between laboratory measured and linear model predicted IDT strengths. Due to the small range of air voids tested in this study, 6.5 – 7.5%, air voids were not found to be significantly correlated to IDT strength. However the importance of accounting for the effect of air voids on IDT strength is recognized and thus is included as a parameter in the linear strength predictive equation.

$$S_t = C1 + C2PM + C3PG_{High} + C4PG_{Low} + C5ANG + C6FAR + C7P_{1/2"} + C8P_{3/8"} + C9P_{\#4} + C10P_{\#8} + C11P_{\#100} + C12P_{\#200} + C13AV \quad (10)$$

The value of the parameter coefficients and the resulting linear model is shown in Equation 11.

$$S_t = -9.901 + 20.737PM + 2.674PG_{High} - 6.407PG_{Low} + .669ANG + 356.593FAR + 1.027P_{1/2"} + 2.517P_{3/8"} - 3.768P_{\#4} + 5.151P_{\#8} + 3.452P_{\#100} - 62.733P_{\#200} - .017AV \quad (11)$$

Where:

- PM = Polymer Modification Factor, either 1 for polymer modified or 0 for unmodified binder
- PG_{High} = Magnitude of high PG
- PG_{Low} = Magnitude of low PG
- ANG = Angularity, %
- FAR = Fines/Asphalt Ratio
- $P_{1/2''}$ = Percent passing the 1/2" sieve
- $P_{3/8''}$ = Percent passing the 3/8" sieve
- $P_{\#4}$ = Percent passing the #4 sieve
- $P_{\#8}$ = Percent passing the #8 sieve
- $P_{\#100}$ = Percent passing the #100 sieve
- $P_{\#200}$ = Percent passing the #200 sieve
- AV = Percent Air Voids

Comparison of the measured versus predicted IDT strength values for the original Pavement ME Design and linear IDT strength models are plotted in Figure 21 and Figure 24, respectively. It is noted that predicted Pavement ME Design IDT strength in Figure 21 is the software output IDT strength, as opposed to prediction by the original IDT equation developed by Witczak et al [6] used in the previous section. The main difference is that binder properties,

ARTFO and *Pen77*, are predicted from PG. For output of IDT strength prediction in Pavement ME Design the PG, design air voids (%), and effective binder content, P_{be} (%) are entered into the design guide software and IDT strength is immediately calculated.

Visual inspection of the original Pavement ME Design IDT strength model shows points are poorly distributed with respect to the LOE while for the linear IDT strength model points are fairly well distributed along the LOE.

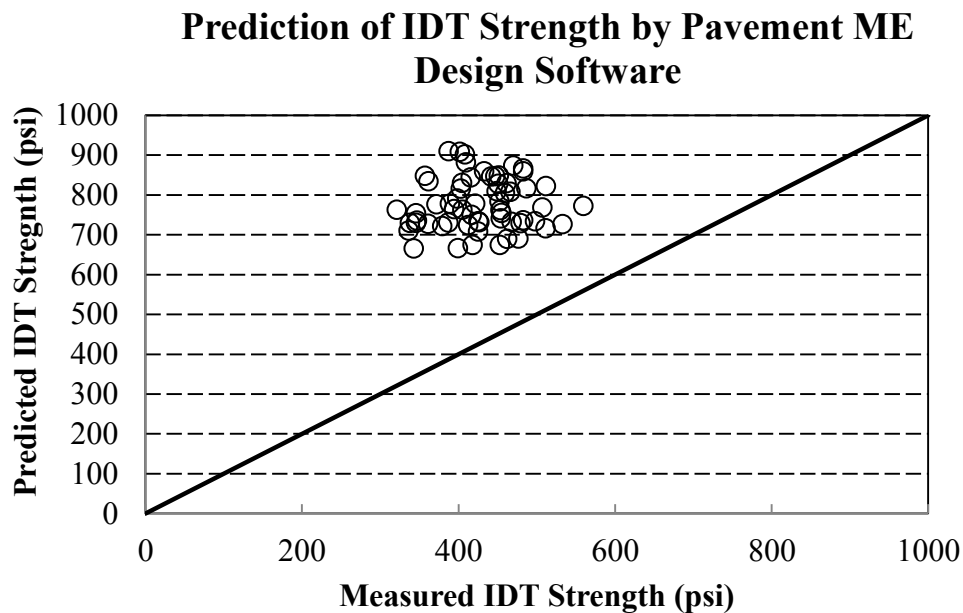


Figure 21 IDT strength predicted by Pavement ME Design software versus laboratory measured IDT strength for commonly used State of Michigan asphalt mixtures

Development of a linear IDT strength predictive model was accomplished using all specimens tested in this study (202 mixtures). A comparison of measured versus predicted IDT strengths for calibration, testing, and all stages is shown in Figure 22, Figure 23, and Figure 24 respectively.

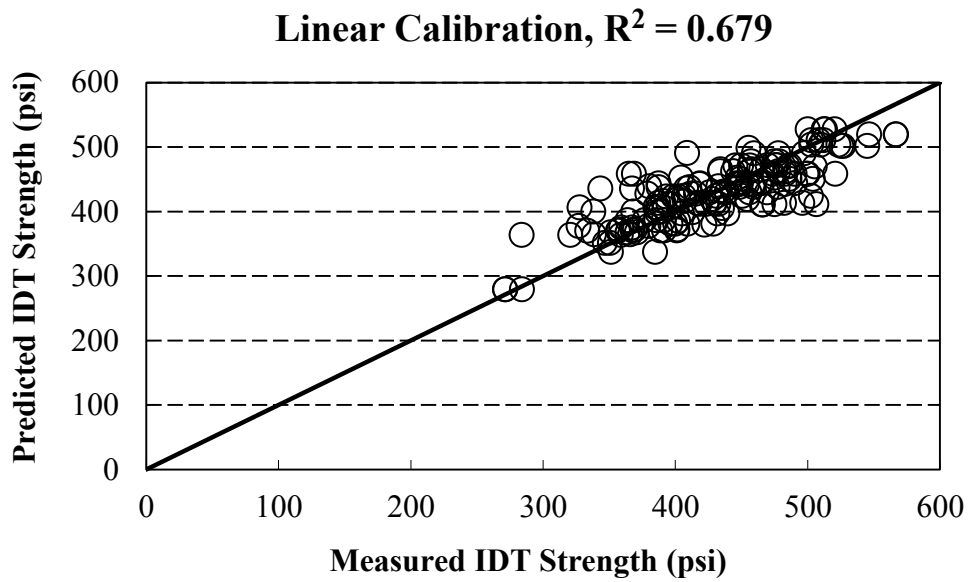


Figure 22 IDT strength predicted during calibration by newly developed linear model versus laboratory measured IDT strength for commonly used State of Michigan asphalt mixtures

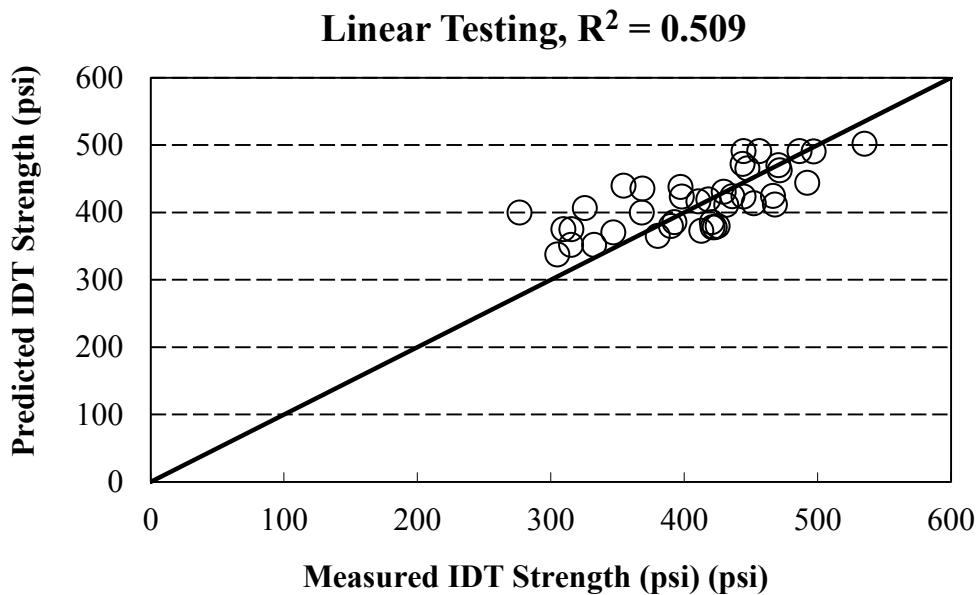


Figure 23 IDT strength predicted during testing by newly developed linear model versus laboratory measured IDT strength for commonly used State of Michigan asphalt mixtures

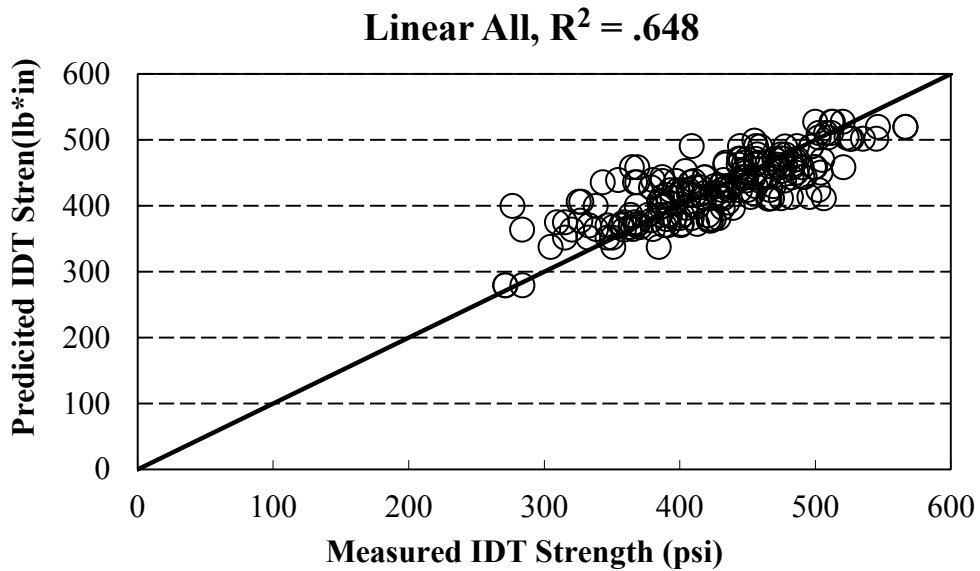


Figure 24 IDT strength predicated for all specimens by newly developed linear model versus laboratory measured IDT strength for commonly used State of Michigan asphalt mixtures

A comparison of model performance evaluation criteria for the original Pavement ME Design and linear IDT strength models are listed in Table 13 along with the number of unique sample used for each stage of development.

Table 13 Comparison of performance criteria for the original Pavement ME Design and linear IDT strength prediction models for commonly used MDOT asphalt mixtures

Model Performance Measure	IDT Predictive Equation			
	Pavement ME	Cal.	Test	All
Unique Samples	62	161	40	201
R ²	0.006	0.679	0.509	0.648
S _e /S _y	6.954	0.594	0.887	0.615

The linear IDT strength model shows increased performance with a lower standard error of estimate/standard deviation, $S_e/S_y = 0.615$, and higher correlation coefficient, $R^2 = 0.648$, as compared to the original Pavement ME Design model. Local bias statistics, unconstrained slope and intercept, of the Michigan calibrated model are 0.69 and 130.24, respectively, indicating a trend of the calibrated model to under predict IDT strength as was seen in the Michigan calibrated Pavement ME Design IDT strength model discussed previously.

5.5 Artificial Neural Network Prediction Model

The third effort to improve Pavement ME Design IDT strength prediction performance was development of an Artificial Neural Network (ANN) using the strength and mix design properties and volumetrics data in this study. An ANN can most simply be defined as a computational model used to predict a desired output from a set of inputs. Unlike regression techniques, the ANN concept is modeled after living neural networks, giving it the capability to learn and recognize patterns. Inputs into an ANN are assigned weights and thresholds which are varied by functions in a network of layers within the ANN. Ultimately the ANN adjusts the weights and thresholds within the layers to predict a desired output. First used in the field of computer science ANNs are now used widely in the field of civil engineering [5], including pavement engineering. In the pavement engineering field ANNs have been employed to successfully estimate pavement layer thickness [15], IDT strength [14], reflective cracking [9], base layer moduli [33], roughness and permeability [11] [32], and rutting and fatigue distresses [19]. Notably, ANN modeling techniques have also been employed in the Pavement ME Design [6].

5.5.1 Structure of the IDT Strength ANN

The ANN developed for the prediction of IDT strength in this study consists of a feed forward (back propagation) network of one hidden layer and one output layer (Figure 25). This structure was determined through a trial and error using the readily available MATLAB neural network toolbox [12].

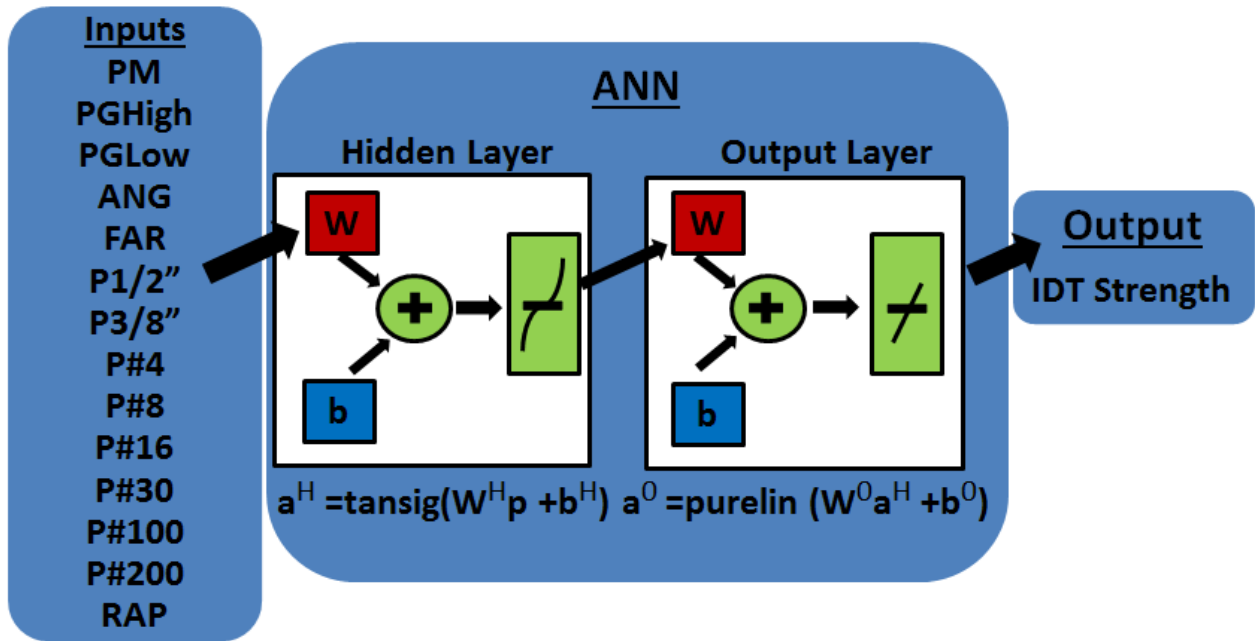


Figure 25 Structure of the ANN model developed for prediction of IDT strength for Michigan asphalt mixtures

5.5.2 Overview of IDT Strength Prediction with the ANN

Forward computation of IDT strength, y , in this ANN model was determined from the following 15 inputs hereby referred to as \mathbf{p} , a 15 x1 input vector. Inputs into the ANN developed as part of this study were the following:

PM = Polymer Modification Factor, either 1 for polymer modified binder or 0 for unmodified binder
 PG_{High} = Magnitude of high PG
 PG_{Low} = Magnitude of low PG
 ANG = Angularity, %
 FAR = Fines/Asphalt Ratio
 $P_{1/2''}$ = Percent passing the 1/2" sieve
 $P_{3/8''}$ = Percent passing the 3/8" sieve
 $P_{\#4}$ = Percent passing the #4 sieve
 $P_{\#8}$ = Percent passing the #8 sieve
 $P_{\#16}$ = Percent passing the #16 sieve
 $P_{\#30}$ = Percent passing the #30 sieve
 $P_{\#100}$ = Percent passing the #100 sieve
 $P_{\#200}$ = Percent passing the #200 sieve
 RAP = Percent Recycled Asphalt Pavement (RAP)
 AV = Percent Air Voids

The process of forward computation in an ANN is completed according to the following steps.

Step 1) The output of the hidden layer, \mathbf{a}^H a 15 x 1 vector, is computed using Equations 12 and 13.

$$\mathbf{n}^H = \mathbf{W}^H \mathbf{p} + \mathbf{b}^H \quad (12)$$

$$\mathbf{a}^H = \text{tansig}(\mathbf{n}^H) \quad (13)$$

Where:

$$\text{tansig}(x) = \frac{2}{1+\exp(-2x)} - 1 \quad (14)$$

And:

\mathbf{W}^H = The matrix weight vector, 12 x 14

\mathbf{b}^H = The bias vector of the hidden layer, 12 x 1

Step 2) With the output hidden layer, \mathbf{a}^H , the output of the output layer, y , is computed using Equation 15 and 16.

$$n^o = \mathbf{W}^o \mathbf{a}^H + b^o \quad (15)$$

$$y = \text{purelin}(n^o) \quad (16)$$

Where:

\mathbf{W}^o = The matrix weight vector, 1 x 12

b^o = The bias constant of the output layer, 12 x 1

5.5.2 Training of the IDT Strength ANN

The ANN was then trained with laboratory measured IDT strength data gathered from testing of all 62 unique MDOT mixtures used in this study. To increase training accuracy,

individual IDT strength tests, generally 3 replicates for each mixture, were used in the ANN training procedure resulting in a total of 183 data points. For the training procedure, weights and biases are varied randomly and repeatedly until the predicted output (i.e. IDT strength) approaches the measured IDT strength, such that difference between the two is minimized. Error minimization is measured as the mean square error between measured and predicted IDT strength and decreases as the number of repetitions increases (Figure 26).

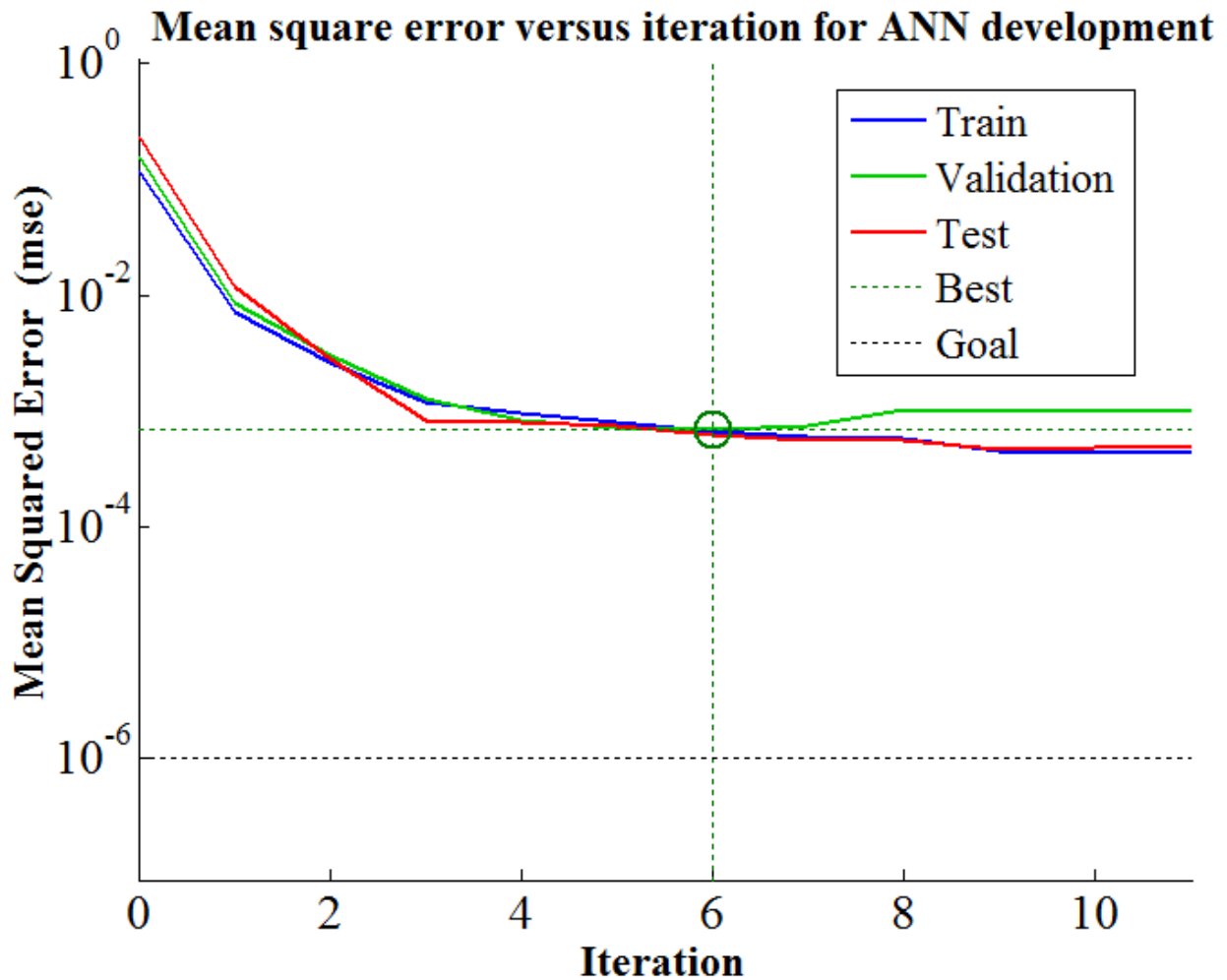


Figure 26 Reduction in mean squared error of laboratory measured and ANN predicted IDT strength values during training, validation, and testing stages of ANN development

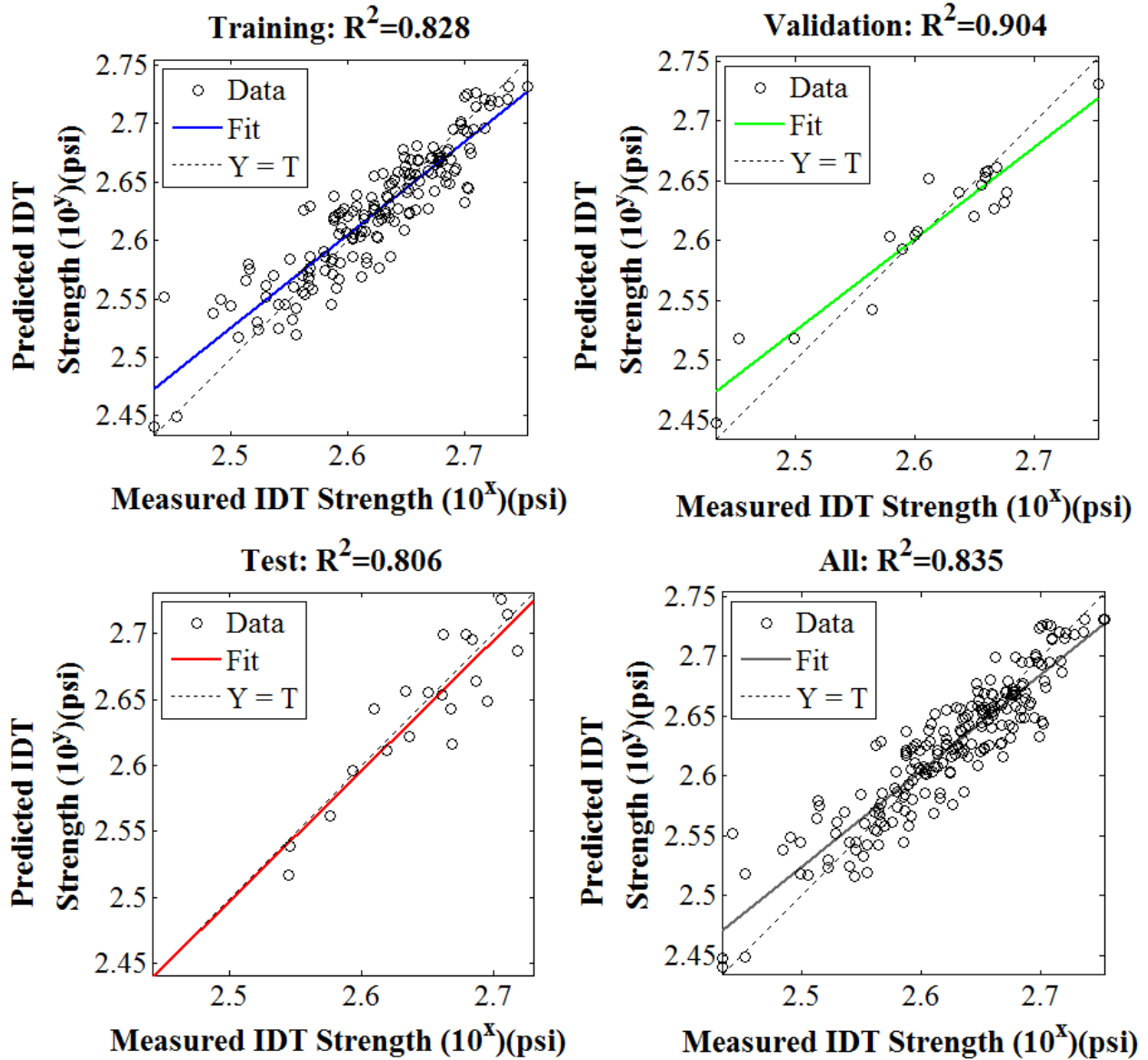


Figure 27 ANN predicted IDT strength versus measured IDT strength (base 10) for the training, validation, testing, and all data used in ANN development

Performance of the trained ANN was evaluated with the goodness-of-fit statistic, R^2 , and visual inspection with respect to the LOE. R^2 for the trained IDT strength ANN was 0.828 and data points were fairly well distributed around the LOE (Figure 27).

5.5.3 Testing of the IDT Strength ANN

Final validation of the IDT strength ANN was completed using 20 individual IDT strength tests set aside from the original 201 strength tests used in the training and validation steps. These 20 tests were input into the IDT ANN feed forward computation model and the predicted versus measured IDT strength values were evaluated (Figure 27). The IDT strength ANN showed an acceptable correlation coefficient, $R^2 = 0.806$, for testing (Figure 27). R^2 for all IDT strength ANN data was 0.835 and data points were fairly well distributed around the LOE (Figure 28). A summary of specimens used and correlation coefficients for each step of ANN development and is shown in Table 14.

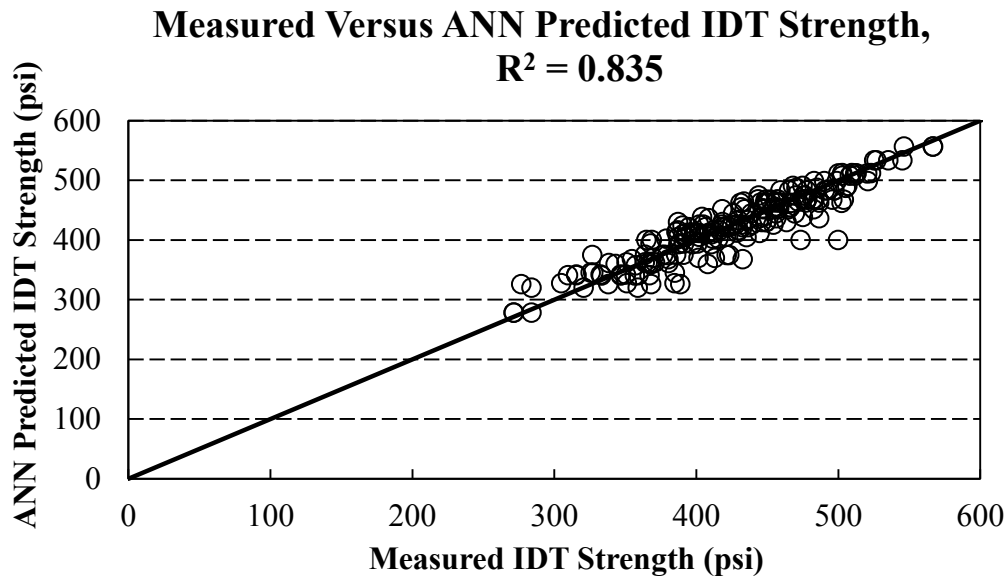


Figure 28 ANN Predicated versus measured IDT strength values for all mixtures used in ANN development

Table 14 Overview of specimens used and correlation coefficients for each stage of IDT ANN development

ANN Development Stage	# Unique Tests	R^2
Training	160	0.828
Validation	21	0.904
Testing	20	0.806
All	201	0.835

6. CONCLUSIONS AND RECOMMENDATIONS

Accurate low temperature material characterization is critical for successful design of flexible pavements such that they resist thermal cracking in the field. The indirect tensile (IDT) strength of an asphalt mixture is an important parameter used in characterization of its thermal cracking resistance. This research investigated the IDT strength characteristics of numerous asphalt mixtures commonly used in the State of Michigan. The research program also included investigation of the ability of Pavement ME Design Guide in predicting IDT strength of the asphalt mixtures from the constituent properties in Level 3 analysis. In an effort to improve IDT strength prediction for use in Pavement ME Design Guide, new IDT strength predictive models were developed. First, the current Pavement ME Design Guide IDT strength predictive model was locally calibrated with the Michigan mixtures tested in this study. Second a new IDT strength predictive model was developed using linear regression techniques. Lastly, an Artificial Neural Network (ANN) was trained and validated using the Michigan mixtures. All inputs in the newly developed and ANN IDT strength models can easily be obtained by designers from mix design Job Mix Formulas (JMFs). Based on the foregoing, the following major conclusions were drawn:

- In 62 different Michigan mixtures tested, a wide variety of IDT strength and fracture work values were observed. The IDT strength and fracture work were affected by factors such as the aggregate gradation, binder PG, and aggregate angularity of the asphalt mixtures.
- Direct relationship between the IDT strength as well as fracture work to binder Performance Grade (PG) and MDOT mixture designation was not observed. Generally, stiff binders resulted in higher low temperature IDT strength and lower fracture work.

- Level 3 IDT strength predictions of Pavement ME Design Guide were very poor for the Michigan asphalt mixtures. All three predictive models developed in this study showed improved IDT strength prediction performance as compared to Pavement ME Design Guide Level 3 IDT strength prediction.

It is recommend that pavement designers in the State of Michigan exercise caution when relying on low PG or MDOT mix designation as a method to increase or decrease IDT strength and when using the IDT strength predictive equation in Pavement ME Design Guide Level 3 thermal cracking analysis. To determine mixture low temperate IDT strength, the models developed in this study should be used instead (depending on the inputs available).

APPENDICES

APPENDIX A: MIX PROPERTIES AND VOLUMETRICS OF MIXTURES TESTED

Table 15 Mixture properties and volumetrics of mixtures tested

Sample ID	Measured Peak Tensile Strength (psi)	Corrected Tensile Strength (psi)	FE Total (lb*in)	FE Pre (lb*in)	FE Post (lb*in)	Polymer Modified (1=yes, 0=no)	PG High Grade	PG Low Grade	RAP (%)	Mix Type	P_b (%) (JMF)
2A	562	477	280	275	5	0	64	22	17	3E30	4.90
2B (WMA)	414	362	419	261	158	0	64	28	17	3E30	4.90
4	570	483	415	300	115	1	70	28	16	4E30	5.31
18A	391	343	365	228	137	0	58	22	19	3E10	5.20
18B	544	463	273	244	30	0	58	22	19	3E10	5.04
20A	530	452	258	255	3	0	64	28	18	4E10	5.23
20B	524	448	341	263	78	0	64	28	20	5E10	5.53
20C	457	395	362	247	115	0	64	28	20	4E10	5.58
21	533	454	281	281	0	0	64	28	21	5E10	6.01
23	542	462	446	320	125	1	70	28	16	4E10 High Stress	4.94
24A	428	372	527	287	240	0	70	28	16	5E10	6.29
24B	589	498	459	335	123	1	70	28	19	5E10	5.78
26A	463	400	412	247	165	0	58	22	19	3E3	5.60
26B	384	338	430	220	210	0	58	28	24	3E3	5.30
26C	394	346	349	247	102	0	58	28	28	3E3	5.43
28A	570	483	225	225	0	0	64	28	21	4E3	5.40
28B	484	416	185	183	2	0	64	28	19	4E3	5.43
29A	462	399	280	260	20	0	64	28	16	5E3	5.99
29B	496	426	202	198	4	0	64	28	21	5E3	5.92
31A	518	442	281	254	27	1	70	28	19	4E3	5.62
31B	553	470	283	279	4	1	70	28	21	4E3	5.40
32A	540	460	327	291	35	1	70	28	16	5E3	5.99
32B	531	453	406	275	131	1	70	28	22	5E3 High Stress	6.08

Table 15 (cont'd)

Sample ID	Measured Peak Tensile Strength (psi)	Corrected Tensile Strength (psi)	FE Total (lb*in)	FE Pre (lb*in)	FE Post (lb*in)	Polymer Modified (1=yes, 0=no)	PG High Grade	PG Low Grade	RAP (%)	Mix Type	P_b (%) (JMF)
44	470	405	226	226	0	0	58	28	25	4E1	5.35
45	395	346	323	252	71	0	58	28	24	5E1	5.98
47	506	433	245	245	0	0	64	28	25	4E1 High Stress	5.29
48	491	422	213	213	0	0	64	28	30	5E1 High Stress	5.91
49A	447	387	499	260	239	1	70	28	0	GGSP	6.18
49B	382	336	1014	200	813	1	70	28	0	GGSP	6.12
51A	396	347	544	226	318	0	58	28	15	LVSP	6.24
51B	470	405	215	215	0	0	58	28	30	LVSP	5.36
51C (WMA)	437	379	294	236	59	0	58	28	15	LVSP	5.60
62	480	413	508	265	243	0	58	28	10	3E3	4.89
64	448	388	246	202	43	0	58	34	19	4E3	5.40
65	415	362	324	274	50	0	58	34	20	5E3	6.00
67	466	402	522	253	269	1	64	34	15	4E3 High Stress	5.10
68	476	410	405	292	112	1	64	34	17	5E3 High Stress	5.46
80	474	409	537	295	241	0	58	34	21	4E1	5.45
81	409	357	193	193	0	0	58	34	20	5E1	5.66
85	467	403	622	254	367	1	64	34	17	4E1 HS	5.48
86	486	417	538	287	251	1	64	34	21	5E1 High Stress	6.14
90	534	455	182	182	0	1	70	22	18	4E30	4.98

Table 15 (cont'd)

Sample ID	Measured Peak Tensile Strength (psi)	Corrected Tensile Strength (psi)	FE Total (lb*in)	FE Pre (lb*in)	FE Post (lb*in)	Polymer Modified (1=yes, 0=no)	PG High Grade	PG Low Grade	RAP (%)	Mix Type	P_b (%) (JMF)
102	575	487	343	297	46	0	64	22	20	4E10	5.20
103	498	427	333	218	115	0	64	22	19	5E10	5.60
105	526	449	312	297	15	1	70	22	14	4E10 High Stress	5.08
108	549	467	302	298	4	0	64	22	20	4E3	5.21
109	566	480	241	241	0	0	64	22	18	5E3	5.50
111	607	512	338	321	16	1	70	22	20	4E3 High Stress	5.31
112	634	533	238	238	0	1	70	22	19	5E3 High Stress	5.80
127	450	389	307	243	64	0	58	22	23	LVSP	5.43
200	570	483	242	242	0	0	58	28	25	3E10	5.20
201	304	276	232	180	52	0	64	28		ASCRL	3.30
202	606	512	185	185	0	0	64	22	21	5E10	6.03
203	529	451	337	289	49	1	70	22	14	4E30 High Stress	4.99
204	668	560	383	377	6	1	70	22	15	5E30 High Stress	5.80
205	363	321				0	58	28	25	2E3	4.90
206	551	468	178	178	0	0	64	22	15	5E1	5.40
208 WMA	496	425	174	174	0	0	64	22	30	LVSP	5.60
209 HMA	532	453	200	200	0	0	64	22	21	5E10	6.21
209 WMA	487	419	196	192	4	0	64	22	21	5E10	6.21

Table 15 (cont'd)

Sample ID	VMA	VFA	% Air	Angularity	G_{mm}	G_{mb}	G_b	G_{se}	G_{sb}	P_{be}	Fines/Asphalt Ratio	Crushed Face 1	1-1/2"
2A	13.9 4	78.4 7	3.00	46.00	2.545	2.469	1.027	2.755	2.728	4.55	1.100	99.60	100.00
2B (WMA)	14.0 2	78.6 7	3.00	46.00	2.508	2.433	1.029	2.708	2.691	-	0.960	98.30	100.00
4	15.0 4	73.5 1	4.00	45.30	2.510	2.410	1.025	2.732	2.686	4.70	1.040	94.90	100.00
18A	14.1 6	78.8 1	3.00	46.00	2.534	2.458	1.018	2.760	2.715	4.62	1.130	99.70	100.00
18B	13.5 2	77.8 1	3.00	41.30	2.502	2.427	1.023	2.710	2.665	-	0.990	92.30	100.00
20A	15.0 5	73.4 9	4.00	45.20	2.506	2.406	1.029	2.722	2.684	4.72	1.000	85.90	100.00
20B	14.9 7	73.2 8	4.00	45.00	2.485	2.386	1.029	2.710	2.651	4.73	1.230	92.30	100.00
20C	14.8 3	76.4 0	3.50	45.20	2.489	2.402	1.032	2.715	2.663	-	0.940	92.70	100.00
21	16.3 4	75.5 8	4.00	45.30	2.481	2.382	1.029	2.727	2.676	5.33	1.010	94.80	100.00
23	14.4 0	75.6 9	3.50	46.00	2.578	2.488	1.030	2.796	2.763	-	0.950	92.70	100.00
24A	16.0 4	75.0 6	4.00	45.40	2.426	2.329	1.031	2.668	2.599	5.33	1.090	95.50	100.00
24B	15.9 4	78.0 4	3.50	45.00	2.531	2.422	1.030	2.779	2.737	-	1.070	86.60	100.00
26A	14.1 7	78.8 3	3.00	45.00	2.538	2.462	1.018	2.785	2.708	4.62	1.130	99.50	100.00
26B	13.8 0	78.1 7	3.00	42.10	2.490	2.415	1.020	2.709	2.653	4.55	0.960	96.90	100.00

Table 15 (cont'd)

Sample ID	VMA	VFA	% Air	Angularity	G_{mm}	G_{mb}	G_b	G_{se}	G_{sb}	P_{be}	Fines/Asphalt Ratio	Crushed Face 1	1-1/2"
28A	14.7 5	72.8 7	4.00	41.20	2.471	2.372	1.028	2.686	2.632	4.66	1.160	90.40	100.00
28B	15.0 6	73.4 4	4.00	41.70	2.490	2.390	1.028	2.711	2.661	4.76	1.070	90.40	100.00
29A	15.7 4	74.5 9	4.00	43.40	2.457	2.359	1.028	2.696	2.632	5.12	1.060	90.60	100.00
29B	16.0 7	75.1 1	4.00	43.00	2.463	2.364	1.028	2.700	2.650	5.24	0.930	76.60	100.00
31A	15.2 7	73.7 6	4.00	41.20	2.471	2.372	1.017	2.701	2.642	4.83	0.970	95.00	100.00
31B	14.7 1	72.8 1	4.00	41.20	2.472	2.373	1.031	2.686	2.632	4.66	1.160	90.40	100.00
32A	15.7 1	74.5 4	4.00	43.40	2.458	2.360	1.031	2.696	2.632	5.12	1.060	90.60	100.00
32B	16.2 0	75.3 1	4.00	41.70	2.450	2.352	1.017	2.696	2.636	5.27	0.950	94.80	100.00
37	16.5 2	75.7 8	4.00	42.60	2.494	2.395	1.032	2.743	2.696	5.39	1.090	93.80	100.00
44	15.0 7	73.4 6	4.00	42.10	2.475	2.376	1.020	2.692	2.648	4.75	0.930	88.50	100.00
45	16.2 2	75.3 8	4.00	42.40	2.454	2.356	1.020	2.695	2.644	5.29	1.020	97.20	100.00
47	14.8 8	73.1 2	4.00	42.60	2.504	2.404	1.029	2.722	2.675	4.66	1.140	85.50	100.00
48	16.0 2	75.0 3	4.00	41.90	2.474	2.375	1.029	2.713	2.661	5.21	1.170	92.80	100.00
49A	17.5 9	77.3 5	4.00	48.90	2.535	2.434	1.025	2.808	2.771	5.72	1.430	100.00	100.00

Table 15 (cont'd)

Sample ID	VMA	VFA	% Air	Angularity	G_{mm}	G_{mb}	G_b	G_{se}	G_{sb}	P_{be}	Fines/Asphalt Ratio	Crushed Face 1	1-1/2"
51A	16.5 1	75.8 0	4.00	-	2.474	2.375	1.032	2.727	2.667	5.44	0.860	98.90	100.00
51B	14.7 2	76.2 2	3.50	-	2.483	2.396	1.024	2.701	2.659	-	1.080	74.70	100.00
51C (WMA)	15.3 7	77.3 3	3.50	-	2.468	2.382	1.024	2.693	2.657	-	0.880	95.40	100.00
62	14.1 7	78.8 2	3.00	42.90	2.589	2.512	1.032	2.807	2.783	4.59	0.760	98.40	100.00
64	15.0 0	73.3 0	4.00	41.00	2.462	2.364	1.023	2.679	2.629	4.74	0.950	75.30	100.00
65	16.1 0	75.2 0	4.00	43.20	2.468	2.369	1.023	2.712	2.655	5.24	0.910	81.80	100.00
67	15.4 0	74.1 0	4.00	42.10	2.565	2.463	1.026	2.789	2.764	4.75	1.050	96.30	100.00
68	15.7 8	75.6 5	4.00	42.80	2.537	2.436	1.026	2.773	2.734	4.96	1.050	94.70	100.00
80	15.2 0	73.7 0	4.00	41.80	2.511	2.411	1.026	2.740	2.688	4.77	1.170	89.30	100.00
81	16.1 1	75.2 0	4.00	42.80	2.523	2.422	1.026	2.765	2.724	5.13	1.130	88.80	100.00
85	15.2 0	77.0 0	3.50	43.20	2.497	2.410	1.033	2.721	2.686	-	1.080	87.70	100.00
86	16.0 0	81.2 0	3.50	42.50	2.471	2.397	1.033	2.718	2.678	-	1.020	75.00	100.00
90	14.7 3	76.2 3	3.50	47.00	2.547	2.458	1.023	2.763	2.739	-	1.200	97.00	100.00
97	15.9	74.8	4.00	46.00	2.537	2.436	1.023	2.776	2.738		1.240	99.80	100.00

Table 15 (cont'd)

Sample ID	VMA	VFA	% Air	Angularity	G_{mm}	G_{mb}	G_b	G_{se}	G_{sb}	P_{be}	Fines/Asphalt Ratio	Crushed Face 1	1-1/2"
102	14.9 6	73.2 5	4.00	46.00	2.550	2.448	1.027	2.776	2.729	4.60	1.220	99.50	100.00
103	16.0 6	75.1 0	4.00	45.00	2.498	2.398	1.027	2.730	2.697	5.17	1.160	92.30	100.00
105	15.2 3	73.7 4	4.00	46.00	2.536	2.434	1.025	2.753	2.726	4.73	1.160	95.50	100.00
108	15.0 5	73.4 3	4.00	46.00	2.541	2.439	1.027	2.765	2.722	4.65	1.220	97.90	100.00
109	16.0 8	75.1 2	4.00	45.00	2.493	2.393	1.027	2.719	2.695	5.18	1.240	98.60	100.00
111	15.0 9	73.5 0	4.00	46.00	2.544	2.443	1.025	2.775	2.724	4.66	1.220	99.20	100.00
112	16.3 9	75.5 9	4.00	45.00	2.489	2.389	1.025	2.729	2.692	5.31	1.150	99.80	100.00
127	15.2 3	73.7 4	4.00	-	2.522	2.421	1.022	2.754	2.701	4.74	1.180	93.50	100.00
200	13.7 0	78.2 2	3.00	43.20	2.513	2.438	1.024	2.731	2.678	4.50	1.130	82.00	100.00
201		-	-	3.30	2.734		1.026	2.835	2.775	2.54	1.090	100.00	100.00
202	16.1 9	75.3 6	4.00	45.60	2.482	2.383	1.031	2.728	2.672	5.29	1.140	95.20	100.00
203	14.8 5	73.0 7	4.00	47.00	2.510	2.410	1.025	2.717	2.689	4.62	1.190	99.30	100.00
204	15.7 7	74.6 3	4.00	47.00	2.524	2.423	1.025	2.774	2.710	4.98	1.230	99.80	100.00
205	13.2 3	77.3 2	3.00	42.10	2.502	2.427	1.020	2.704	2.660	4.31	1.052	95.90	100.00

Table 15 (cont'd)

Sample ID	VMA	VFA	% Air	Angularity	G_{mm}	G_{mb}	G_b	G_{se}	G_{sb}	P_{be}	Fines/Asphalt Ratio	Crushed Face 1	1-1/2"
206	16.0 8	75.1 3	4.00	45.00	2.503	2.403	1.027	2.727	2.709	5.16	1.250	97.90	100.00
208 WMA	14.7 5	76.2 7	3.50	-	2.461	2.375	1.034	2.680	2.630	-	0.920	85.00	100.00
209 HMA	15.8 9	77.9 7	3.50	45.00	2.476	2.389	1.209	2.730	2.664	-	0.920	95.00	100.00
209 WMA	15.8 9	77.9 7	3.50	45.00	2.476	2.389	1.209	2.730	2.664	-	0.920	95.00	100.00

Table 15 (cont'd)

Sample ID	1"	3/4"	1/2"	3/8"	No. 4	No. 8	No. 16	No. 30	No. 50	No. 100	No. 200
2A	100.00	100.00	83.00	72.30	47.30	34.90	26.00	18.20	9.30	6.10	5.00
2B (WMA)	100.00	100.00	88.10	77.10	57.60	40.90	27.70	19.50	12.70	7.50	4.50
4	100.00	100.00	98.80	88.60	73.20	56.30	38.00	25.20	14.70	7.80	4.90
18A	100.00	100.00	84.50	73.40	49.40	34.70	25.70	20.20	11.50	6.90	5.20
18B	100.00	98.10	88.80	84.30	65.80	46.20	33.90	25.50	16.30	7.40	4.40
20A	100.00	100.00	98.80	89.50	71.10	53.50	36.30	23.50	13.10	7.40	4.70
20B	100.00	100.00	93.40	90.40	83.40	56.20	36.70	25.60	15.80	8.40	5.80
20C	100.00	100.00	93.20	88.60	73.50	54.00	40.70	30.80	19.40	8.60	4.60
21	100.00	100.00	100.00	99.20	83.60	66.30	46.50	31.20	17.30	8.70	5.40
23	100.00	100.00	91.60	83.00	68.30	50.00	35.90	25.60	14.40	6.80	4.30
24A	100.00	100.00	100.00	95.70	80.10	58.00	39.90	28.70	16.20	7.70	5.80
24B	100.00	100.00	100.00	97.80	86.80	61.80	44.30	32.30	18.30	9.00	5.60
26A	100.00	100.00	88.10	78.40	52.60	33.00	22.10	15.60	10.90	7.20	5.20
26B	100.00	100.00	89.80	80.70	63.60	46.30	35.60	26.60	13.90	6.50	4.40
26C	100.00	100.00	86.10	80.70	63.30	49.00	41.40	32.60	14.20	6.20	4.50
28A	100.00	100.00	98.90	89.60	71.50	57.00	46.30	35.90	15.60	7.00	5.40
28B	100.00	100.00	90.10	84.40	71.20	55.70	44.20	32.20	16.10	7.40	5.10
29A	100.00	100.00	100.00	97.90	80.30	59.60	44.90	32.90	15.20	7.20	5.40
29B	100.00	100.00	100.00	96.90	77.40	59.00	46.40	33.20	16.10	7.10	4.90
31A	100.00	100.00	93.90	87.80	72.00	56.70	43.90	32.60	16.30	6.90	4.70
31B	100.00	100.00	98.90	89.60	71.50	57.00	46.30	35.90	15.60	7.00	5.40
32A	100.00	100.00	100.00	97.90	80.30	59.60	44.90	32.90	15.20	7.20	5.40
32B	100.00	100.00	100.00	96.70	77.80	58.20	45.10	34.20	191.00	7.40	5.00
37	100.00	100.00	100.00	92.50	70.10	58.60	50.30	41.10	21.90	8.70	5.90
44	100.00	100.00	93.70	86.20	73.30	54.80	41.80	30.60	16.10	6.60	4.40
45	100.00	100.00	100.00	96.60	77.40	57.80	45.10	34.40	18.60	8.00	5.40
47	100.00	100.00	93.50	87.10	76.40	57.20	41.30	29.90	16.60	8.00	5.30

Table 15 (cont'd)

Sample ID	1"	3/4"	1/2"	3/8"	No. 4	No. 8	No. 16	No. 30	No. 50	No. 100	No. 200
48	100.00	100.00	100.00	99.70	83.30	63.00	49.80	36.70	20.00	9.20	6.10
49A	100.00	100.00	94.60	70.00	26.60	20.50	16.60	13.00	10.40	8.90	8.20
49B	100.00	100.00	96.10	79.70	31.80	22.10	17.80	14.40	11.80	9.70	8.10
51A	100.00	100.00	94.80	83.20	58.70	44.60	35.90	27.40	14.00	7.10	4.70
51B	100.00	100.00	91.90	84.80	72.40	57.20	45.40	35.50	19.50	7.90	5.20
51C (WMA)	100.00	100.00	91.20	85.70	71.40	56.70	43.90	30.80	14.80	7.30	4.50
62	100.00	100.00	86.50	76.10	56.90	45.40	34.40	23.10	14.60	6.10	3.50
64	100.00	100.00	95.00	86.90	72.50	56.70	43.50	32.20	15.50	6.20	4.50
65	100.00	100.00	100.00	97.40	75.20	56.70	42.50	31.10	15.50	6.60	4.80
67	100.00	100.00	95.90	84.30	64.80	56.20	45.00	30.90	20.10	8.20	5.00
68	100.00	100.00	100.00	95.40	73.60	59.90	47.80	33.90	21.60	8.80	5.20
80	100.00	100.00	98.20	89.90	69.30	54.00	41.10	30.00	18.60	8.40	5.60
81	100.00	100.00	100.00	97.40	75.20	56.40	43.60	31.00	16.80	8.60	5.80
85	100.00	100.00	93.70	84.40	66.40	53.50	42.60	26.90	11.20	7.00	5.40
86	100.00	100.00	100.00	97.00	80.20	62.20	47.80	33.80	18.20	8.20	5.70
90	100.00	100.00	98.20	85.60	63.60	44.20	31.00	22.00	14.00	7.50	5.60
97	100.00	100.00	100.00	99.70	77.70	53.90	37.20	26.20	14.80	9.10	6.20
102	100.00	100.00	98.50	88.60	65.10	45.00	30.30	21.50	13.50	7.80	5.60
103	100.00	100.00	100.00	99.90	75.90	54.70	39.10	29.50	18.00	9.80	6.00
105	100.00	100.00	99.30	88.30	63.00	42.20	28.10	19.40	12.90	7.70	5.50
108	100.00	100.00	98.70	87.30	65.10	46.50	32.30	23.30	14.90	8.10	5.70
109	100.00	100.00	100.00	99.60	75.60	51.40	36.50	27.40	17.60	9.60	6.40
111	100.00	100.00	98.90	87.60	66.50	47.30	33.90	24.40	15.80	8.20	5.70
112	100.00	100.00	100.00	99.90	75.80	54.90	39.20	29.10	18.20	8.40	6.10
127	100.00	100.00	92.50	86.80	79.20	58.50	43.20	32.60	20.90	10.30	5.60
200	100.00	99.90	88.90	82.60	65.00	48.40	34.10	22.50	12.00	7.30	5.10
201	100.00	96.00	59.50	30.20	14.70	11.50	9.10	7.20	6.00	4.60	3.60
202	100.00	100.00	100.00	99.70	84.10	66.70	46.80	31.50	16.60	8.70	6.00
203	100.00	100.00	96.40	87.10	52.30	33.60	22.40	15.90	10.90	7.10	5.50

Table 15 (cont'd)

Sample ID	1"	3/4"	1/2"	3/8"	No. 4	No. 8	No. 16	No. 30	No. 50	No. 100	No. 200
205	100.00	90.00	73.50	69.70	57.40	44.50	35.30	25.50	12.60	5.90	4.40
206	100.00	100.00	100.00	99.70	78.00	53.90	38.60	29.10	18.00	9.60	6.40
208 WMA	100.00	100.00	94.20	86.10	65.20	48.70	39.40	32.40	15.60	6.40	4.50
209 HMA	100.00	100.00	100.00	97.80	77.60	52.70	37.40	25.90	14.20	7.30	4.90
209 WMA	100.00	100.00	100.00	97.80	77.60	52.70	37.40	25.90	14.20	7.30	4.90

APPENDIX B: IDT STRENGTH, FRACTURE WORK, AND VOLUMTERICS OF SPECIMENS TESTED

Table 16 IDT Strength, Fracture Work, and Air Voids of Specimens Tested

Mix	Sample	V_A (%)	IDT Strength (psi)	IDT Strength Average (psi)	SD (psi)	CV (%)	Total FE (lb*in.)	Total FE Average (lb*in)	Total FE SD (lb*in)
2A	2A-1-A	7.6	452.5	477	22.19	4.65	291.0	280	74.63
	2A-3-A	7.3	495.9				349.2		
	2A-1-B	7.2	482.2				201.0		
2B	2B-2-A	6.6	380.5	362	21.28	5.88	392.7	419	91.98
	2B-3-B	7.4	365.8				521.7		
	2B-2-C	7.1	338.5				343.6		
4	4-1-A	7.1	497.2	483	18.13	3.75	359.5	415	53.42
	4-3-A	7.1	459.5				419.0		
	4-1-B	7.1	478.0				-		
	4-3-B	6.9	497.3				466.1		
18A	18-2-2	7.4	276.8	343	48.81	14.2 3	-	365	163.8 5
	18-1-B	7.4	338.1				387.6		
	18-1-C	6.4	368.4				191.2		
	18-3-C	6.6	388.8				516.5		
18B	18B-2-A	6.7	450.4	463	30.26	6.54	387.2	273	87.41
	18B-1-B	6.4	466.8				290.3		
	18B-2-B	7.3	431.2				232.5		
	18B-3-B	7.4	502.6				183.8		
20A	20A-3-A	7.0	454.5	452	32.24	7.14	338.7	269	60.82
	20A-1-B	7.1	418.4				227.5		
	20A-3-B	7.1	482.8				240.4		
20B	20B-1-A	6.6	438.8	448	19.15	4.28	336.0	341	23.58
	20B-3-A	7.4	469.5				309.1		
	20B-1-B	6.8	456.2				361.1		
	20B-3-B	7.0	425.9				356.0		

Table 16 (cont'd)

Mix	Sample	VA (%)	IDT Strength (psi)	IDT Strength Average (psi)	SD (psi)	CV (%)	Total FE (lb*in.)	Total FE Average (lb*in)	Total FE SD (lb*in)
20C	20C-1-A	7.4	369.6	395	22.55	5.71	430.2	362	86.00
	20C-3-A	7.4	401.6				265.6		
	20C-3-B	7.2	413.1				391.0		
21	21-3-B	7.4	472.0	454	19.19	4.23	301.6	281	42.12
	21-1-B	7.3	456.4				309.1		
	21-1-D	7.2	433.8				232.7		
23	23A-1-A	6.7	459.0	462	14.50	3.14	430.2	446	63.20
	23A-2-A	7.5	448.6				515.0		
	23A-3-A	6.7	477.3				391.4		
24A	24-1-B	6.6	343.4	372	26.90	7.23	565.6	527	68.00
	24-3-B	6.8	367.3				602.9		
	24A-1-A	6.6	408.3				477.1		
	24A-3-A	6.9	368.9				462.8		
24B	24B-3-A	7.1	483.2	498	16.39	3.29	441.6	459	84.25
	24B-1-A	7.0	490.2				403.2		
	24B-1-B	7.5	520.9				407.3		
	24B-3-B	6.9	499.1				582.3		
26A	26A-1-A	7.7	413.1	400	19.05	4.77	412.0	412	0.00
	26A-1-B	7.4	386.1				-		

Table 16 (cont'd)

Mix	Sample	VA (%)	IDT Strength (psi)	IDT Strength Average (psi)	SD (psi)	CV (%)	Total FE (lb*in.)	Total FE Average (lb*in)	Total FE SD (lb*in)
26B	26B-1-B	7.5	315.6	338	29.48	8.72	435.0	430	11.29
	26B-3-B	7.7	359.2				418.6		
	26B-2-C	7.3	309.8				422.4		
	26B-3-C	7.7	367.3				443.0		
26C	26C-1-A	7.2	347.0	346	11.77	3.40	417.5	349	62.66
	26C-2-A	7.2	333.4				294.5		
	26C-3-A	6.5	356.8				335.4		
28A	28A-1-A	7.5	492.4	483	15.11	3.13	192.1	225	44.97
	28A-1-B	7.2	490.7				206.3		
	28A-3-B	7.3	465.4				276.1		
28B	28B-1-A	7.1	429.6	416	20.16	4.85	192.8	185	32.71
	28B-3-A	7.5	416.7				222.7		
	28B-1-B	7.4	430.1				143.6		
	28B-3-B	7.2	387.1				182.3		
29A	29A-3-A	7.4	410.7	399	11.65	2.92	276.5	280	11.20
	29A-3-B	7.3	387.5				292.3		
	29A-1-B	7.3	397.4				270.7		

Table 16 (cont'd)

Mix	Sample	VA (%)	IDT Strength (psi)	IDT Strength Average (psi)	SD (psi)	CV (%)	Total FE (lb*in.)	Total FE Average (lb*in)	Total FE SD (lb*in)
29B	29B-1-A	6.7	454.5	426	21.9 4	5.15	169.5	202	23.31
	29B-2-A	7.3	402.1				212.2		
	29B-1-B	6.9	418.5				202.2		
	29B-3-B	7.2	427.9				223.7		
31A	31A-1-A	6.6	475.1	442	35.6 7	8.07	210.7	281	71.88
	31A-2-A	7.1	404.3				279.3		
	31A-3-A	6.5	447.2				354.4		
31B	31B-3-A	6.9	474.9	470	11.2 5	2.39	307.5	283	31.62
	31B-1-A	7.4	478.4				247.4		
	31B-1-B	7.2	457.4				294.6		
32A	32A-1-A	7.0	449.8	460	18.6 1	4.05	316.4	327	41.99
	32A-2-A	7.7	445.5				345.0		
	32A-1-B	6.9	486.7				273.9		
	32A-3-B	7.0	456.3				372.1		
32B	32B-1-A	7.1	458.6	453	8.15	1.80	350.0	406	79.50
	32B-3-A	6.9	447.1				462.4		
37	37-3-B	7.4	431.8	455	19.7 2	4.34	603.9	515	153.9 2
	37-2-1A	7.1	465.4				603.9		
	37-1-B	7.6	466.4				337.3		

Table 16 (cont'd)

Mix	Sample	VA (%)	IDT Strength (psi)	IDT Strength Average (psi)	SD (psi)	CV (%)	Total FE (lb*in.)	Total FE Average (lb*in)	Total FE SD (lb*in)
44	44A-1-C	6.6	387.2	405	26.55	6.56	200.2	226	44.80
	44A-3-C	6.7	435.4				200.3		
	44A-2-C	7.5	392.1				277.8		
45	45-3-A	7.6	325.7	346	33.71	9.74	319.2	323	39.73
	45-1-A	7.1	327.6				364.6		
	45-1-B	6.8	385.0				285.5		
47	47-1-A	6.7	436.2	433	4.45	1.03	215.0	245	41.76
	47-2-A	7.6	429.9				274.1		
48	48-1-A	7.3	436.4	422	21.10	5.01	179.1	213	47.67
	48-3-A	7.3	406.6				246.5		
49A	49A-2-A	7.5	367.9	387	14.01	3.62	414.3	499	140.70
	49A-3-A	6.7	388.7				371.4		
	49A-1-B	6.4	401.1				521.4		
	49A-3-B	7.1	391.5				687.2		
49C	49C-2-A	7.0	332.8	336	15.94	4.74	1295	1014	257.63
	49C-3-A	6.6	346.9				-		
	49C-1-B	7.4	350.6				789.4		
	49C-3-B	7.4	315.5				956.5		
51A	51A-1-A	7.5	305.0	347	40.02	11.53	692.1	544	130.05
	51A-3-A	7.2	384.7				450.1		
	51A-2-A	7.5	351.3				488.7		

Table 16 (cont'd)

Mix	Sample	VA (%)	IDT Strength (psi)	IDT Strength Average (psi)	SD (psi)	CV (%)	Total FE (lb*in.)	Total FE Average (lb*in)	Total FE SD (lb*in)
51B	51B-2-A	7.2	402.1	405	14.2 8	3.52	270.0	215	47.31
	51B-1-B	7.1	421.0				185.4		
	51B-3-B	6.6	393.0				191.1		
51C	51C-1-A	7.6	376.9	379	11.8 9	3.13	321.4	294	26.60
	51C-3-A	7.3	391.2				304.5		
	51C-1-B	7.1	364.0				258.5		
	51C-3-B	7.0	385.8				293.1		
62	62-1-A	6.4	390.4	413	19.2 7	4.67	434.5	508	96.68
	62-3-A	7.0	425.3				617.5		
	62-2-B	7.3	422.0				472.0		
64	64-3-1	7.6	423.3	388	45.3 7	11.7 0	163.0	246	76.78
	64A-1-E	6.6	421.6				208.5		
	64A-3-E	6.6	379.6				339.4		
	64A-1-D	7.5	326.9				271.8		
65	65-1-A	6.9	371.0	362	10.1 0	2.79	369.2	324	40.40
	65-2-A	7.5	351.1				291.4		
	65-3-A	7.0	363.9				311.4		
76	67-1/4-1A	6.6	415.6	402	20.0 9	5.00	451.4	522	85.32
	67-1/4-3	6.7	411.6				498.2		
	67-1/4-2	7.4	379.0				616.9		
68	68-3-B	7.5	402.1	410	23.6 8	5.78	370.4	405	40.21
	68-1-B	7.2	444.8				373.9		
	68-1-D	7.1	393.2				454.6		
	68-3-D	7.5	398.6				420.2		

Table 16 (cont'd)

Mix	Sample	VA (%)	IDT Strength (psi)	IDT Strength Average (psi)	SD (psi)	CV (%)	Total FE (lb*in.)	Total FE Average (lb*in)	Total FE SD (lb*in)
80	80-1-A	6.4	428.8	409	14.5 2	3.55	552.7	514	95.58
	80-2-A	7.1	400.0				628.7		
	80-1-B	7.1	409.1				463.4		
	80-3-B	7.1	396.4				413.0		
81	81-1-1	7.4	357.4	357	0.00	0.00	192.9	193	0.00
85	85A-3-A	7.5	407.2	403	10.6 8	2.65	506.5	622	147.4 8
	85A-1-B	6.8	411.0				570.7		
	85A-3-B	7.4	390.9				787.9		
86	86A-1-A	7.6	432.6	417	16.0 7	3.85	490.0	538	116.3 5
	86A-3-A	7.4	423.4				411.8		
	86A-2-B	6.8	418.4				565.8		
	86A-3-B	6.8	394.9				685.1		
90A	90A-1-B	6.4	455.3	455	0.00	0.00	181.6	182	0.00
97	97A-1-A	6.8	511.9	508	4.53	0.89	225.8	258	28.31
	97A-2-A	7.8	502.9				278.9		
	97A-3-A	7.1	508.2				269.3		
102	102A-3-B	6.4	470.8	487	17.4 0	3.57	281.0	343	80.52
	102A-1-C	6.5	505.4				314.0		
	102A-3-C	6.8	485.1				434.0		

Table 16 (cont'd)

Mix	Sample	VA (%)	IDT Strength (psi)	IDT Strength Average (psi)	SD (psi)	CV (%)	Total FE (lb*in.)	Total FE Average (lb*in)	Total FE SD (lb*in)
103	103A-1-B	6.7	364.9	427	70.1 6	16.4 4	634.1	333	211.6 4
	103A-2-B	7.1	368.8				326.0		
	103A-3-E	7.6	500.1				200.2		
	103A-1-E	7.6	473.7				171.7		
105	105A-2-B	7.5	409.0	449	32.1 2	7.15	387.9	312	58.18
	105A-3-B	6.5	486.6				255.4		
	105A-1-C	7.1	444.7				280.2		
	105A-3-C	7.4	456.5				325.5		
108	108-1-B	7.4	476.7	467	15.3 3	3.29	272.4	302	64.87
	108A-1-B	6.5	475.6				297.1		
	108A-2-B	7.3	470.0				393.1		
	108A-3-B	7.2	444.0				243.5		
109	109-4/2	7.6	449.0	480	28.0 9	5.85	206.8	241	46.34
	109-1-A	6.9	504.1				222.4		
	109-3-A	7.3	486.3				293.7		
111	111A-1-B	6.5	509.7	512	10.3 7	2.03	330.0	338	9.25
	111A-2-B	7.5	523.2				334.7		
	111A-3-B	6.7	502.9				347.9		
112	112-1-A	7.0	545.2	533	9.03	1.69	211.4	238	19.56
	112-3-A	7.2	535.4				252.0		
	112-1-B	7.1	527.1				234.6		
	112-3-B	7.5	525.6				253.3		

Table 16 (cont'd)

Mix	Sample	VA (%)	IDT Strength (psi)	IDT Strength Average (psi)	SD (psi)	CV (%)	Total FE (lb*in.)	Total FE Average (lb*in)	Total FE SD (lb*in)
127	127-1-B	7.3	432.7	389	39.7 2	10.2 0	200.8	307	97.67
	127-3-B	7.4	354.8				393.2		
	127-1-C	7.3	380.5				326.5		
200	200-1-A	7.0	506.6	483	20.4 6	4.23	252.9	242	11.39
	200-3-A	7.3	475.0				242.5		
	200-1-B	7.2	468.2				230.2		
201	201A-1-A	10.8	271.4	276	7.29	2.65	323.7	232	82.95
	201A-2-A	11.6	271.6				163.0		
	201A-3-A	10.6	284.1				207.9		
202	202A-2-A	6.6	513.1	512	8.40	1.64	172.6	185	21.12
	202A-3-A	7.2	500.2				194.9		
	202A-1-B	6.6	512.2				162.8		
	202A-3-B	7.0	520.5				209.3		
203	203-1-A	7.3	447.7	451	13.3 1	2.95	272.9	337	59.69
	203-3-A	7.4	464.9				311.3		
	203A-1-A	7.0	457.5				353.3		
	203A-3-A	7.1	434.1				412.2		
204	204-1-3	7.3	566.8	560	11.7 0	2.09	366.4	383	70.27
	204-1-1	7.3	546.5				322.6		
	204A-3-A	7.5	566.7				460.1		
205	205-2-1	7.0	359.0	321	37.4 9	11.6 7	-	-	-
	205-2-2	7.1	284.0				-		
	205-2-3	7.5	320.7				-		
206	206-1-A	7.3	483.4	468	21.5 2	4.60	201.3	178	20.35
	206-3-A	7.0	477.9				167.7		
	206-1-B	7.5	443.7				164.6		

Table 16 (cont'd)

Mix	Sample	VA (%)	IDT Strength (psi)	IDT Strength Average (psi)	SD (psi)	CV (%)	Total FE (lb*in.)	Total FE Average (lb*in)	Total FE SD (lb*in)
208	208A-1-A	6.6	431.9	425	18.0 9	4.25	158.3	174	22.21
	208A-2-A	7.3	439.4				-		
	208A-3-A	7.0	405.0				189.7		
209 A	209A-3-A	7.1	463.6	453	9.23	2.04	154.5	200	40.93
	209A-1-B	7.2	449.3				212.7		
	209A-3-B	7.4	446.4				233.4		
209 B	209B-1-B	6.8	418.7	419	31.0 6	7.42	244.3	196	51.92
	209B-1-A	7.6	387.4				141.0		
	209B-3-B	7.3	449.5				202.0		

Table 16 (cont'd)

Mix	Total FE CV (%)	Pre FE (lb*in.)	Pre FE Average (lb*in)	Pre FE SD (lb*in)	Pre FE CV (%)	Post FE (lb*in.)	Post FE Average (lb*in)	Post FE SD (lb*in)	Post FE CV (%)
2A	26.62	291.0	275	67.79	24.63	0.0	5	8.84	173.21
		333.8				15.3			
		201.0				0.0			
2B	21.94	281.9	261	29.47	11.28	110.8	158	77.35	48.92
		274.3				247.4			
		227.5				116.1			
4	12.88	282.4	300	29.64	9.87	77.1	115	32.47	28.35
		284.0				135.0			
		334.5				131.6			
18A	44.88	262.1	228	35.52	15.59	125.5	137	143.59	104.58
		191.2				0.0			
		230.1				286.5			
18B	31.96	290.7	244	46.69	19.14	96.4	30	45.76	154.93
		268.6				21.7			
		232.5				0.0			
		183.8				0.0			
20A	22.62	324.9	264	52.91	20.02	13.8	5	7.96	173.21
		227.5				0.0			
		240.4				0.0			
20B	6.92	236.7	263	37.40	14.23	99.3	78	27.24	35.03
		235.3				73.9			
		263.9				97.2			
		315.3				40.7			
20C	23.74	216.3	247	33.44	13.53	213.9	115	95.59	83.04
		242.5				23.1			
		282.7				108.3			
21	14.98	301.6	281	42.12	14.98	0.0	0	0.00	0.00
		309.1				0.0			
		232.7				0.0			
23	14.19	323.7	320	3.92	1.23	106.5	125	61.48	49.07
		321.0				194.0			
		316.0				75.4			
24A	12.90	300.6	287	17.22	6.01	265.0	240	77.69	32.32
		263.3				339.6			
		298.7				178.4			
		284.1				178.6			

Table 16 (cont'd)

Mix	Total FE CV (%)	Pre FE (lb*in.)	Pre FE Average (lb*in)	Pre FE SD (lb*in)	Pre FE CV (%)	Post FE (lb*in.)	Post FE Average (lb*in)	Post FE SD (lb*in)	Post FE CV (%)
24B	18.37	320.4	335	17.31	5.16	121.2	123	89.72	72.81
		328.3				74.9			
		360.2				47.0			
		332.6				249.7			
26A	0.00	246.7	247	0.00	0.00	165.3	165	0.00	0.00
26B	2.63	221.7	220	16.73	7.60	213.3	210	7.51	3.58
		210.9				207.7			
		205.1				217.3			
		243.1				200.0			
26C	17.95	258.0	247	22.92	9.29	159.5	102	49.36	48.16
		220.3				74.2			
		261.6				73.8			
28A	20.00	192.1	225	44.97	20.00	0.0	0	0.00	0.00
		206.3				0.0			
		276.1				0.0			
28B	17.65	192.8	183	29.38	16.05	0.0	2	4.56	200.00
		213.6				9.1			
		143.6				0.0			
		182.3				0.0			
29A	4.00	276.5	260	24.41	9.40	0.0	20	35.03	173.21
		231.6				60.7			
		270.7				0.0			
29B	11.54	169.5	198	20.33	10.29	0.0	4	5.30	122.18
		212.2				0.0			
		195.6				6.6			
		212.9				10.8			
31A	25.53	210.7	254	38.48	15.15	0.0	27	37.48	136.50
		267.1				12.2			
		284.3				70.2			
31B	11.17	296.0	279	27.64	9.90	11.5	4	6.65	173.21
		247.4				0.0			
		294.6				0.0			
32A	12.85	316.4	291	20.34	6.98	0.0	35	40.90	115.53
		275.9				69.1			
		273.9				0.0			
		299.6				72.5			
32B	19.57	249.0	275	36.93	13.42	101.0	131	42.57	32.47
		301.2				161.2			

Table 16 (cont'd)

Mix	Total FE CV (%)	Pre FE (lb*in.)	Pre FE Average (lb*in)	Pre FE SD (lb*in)	Pre FE CV (%)	Post FE (lb*in.)	Post FE Average (lb*in)	Post FE SD (lb*in)	Post FE CV (%)
37	29.89	221.5	254	55.79	21.99	382.4	261	209.70	80.26
		221.5				382.4			
		318.1				19.1			
44	19.82	200.2	226	44.80	19.82	0.0	0	0.00	0.00
		200.3				0.0			
		277.8				0.0			
45	12.29	250.8	252	2.04	0.81	68.5	71	41.35	58.18
		251.0				113.7			
		254.4				31.1			
47	17.07	215.0	245	41.76	17.07	0.0	0	0.00	0.00
		274.1				0.0			
48	22.40	179.1	213	47.67	22.40	0.0	0	0.00	0.00
		246.5				0.0			
49A	28.22	249.4	260	12.63	4.86	164.9	239	144.11	60.37
		277.1				94.2			
		251.6				269.9			
		261.4				425.8			
49C	25.42	220.4	200	24.30	12.14	1074.6	813	247.40	30.41
		206.8				582.6			
		173.2				783.2			
51A	23.92	193.9	226	28.75	12.73	498.2	318	156.72	49.33
		234.1				215.9			
		249.6				239.0			
51B	21.96	270.0	215	47.31	21.96	0.0	0	0.00	0.00
		185.4				0.0			
		191.1				0.0			
51C	9.04	262.2	236	23.97	10.17	59.2	59	14.46	24.58
		249.5				55.0			
		215.4				43.1			
		215.2				77.9			
62	19.03	302.8	265	36.18	13.68	131.7	243	130.31	53.52
		230.9				386.6			
		259.8				212.1			
64	31.25	163.0	202	41.52	20.51	0.0	43	50.06	115.86
		208.5				0.0			
		258.1				81.4			
		180.3				91.5			

Table 16 (cont'd)

Mix	Total FE CV (%)	Pre FE (lb*in.)	Pre FE Average (lb*in)	Pre FE SD (lb*in)	Pre FE CV (%)	Post FE (lb*in.)	Post FE Average (lb*in)	Post FE SD (lb*in)	Post FE CV (%)
65	12.47	264.7	274	8.47	3.09	104.5	50	48.84	98.45
		280.5				10.9			
		278.0				33.5			
76	16.34	245.2	253	34.81	13.75	206.2	269	108.15	40.20
		291.2				207.0			
		223.0				393.9			
68	9.93	287.4	292	25.93	8.87	82.9	112	48.28	42.97
		313.1				60.8			
		311.3				143.3			
		257.7				162.5			
80	18.58	299.5	294	31.73	10.81	253.2	221	123.01	55.70
		248.3				380.3			
		322.3				141.1			
		304.2				108.8			
81	0.00	192.9	193	0.00	0.00	0.0	0	0.00	0.00
85	23.72	273.1	254	30.63	12.05	233.4	367	177.70	48.37
		270.8				299.9			
		219.0				569.0			
86	21.62	293.7	287	33.48	11.67	196.3	251	147.90	58.87
		316.8				95.1			
		298.3				267.5			
		239.0				446.0			
90A	0.00	181.6	182	0.00	0.00	0.0	0	0.00	0.00
97	10.97	225.8	258	28.31	10.97	0.0	0	0.00	0.00
		278.9				0.0			
		269.3				0.0			
102	23.48	281.0	297	28.01	9.43	0.0	46	53.45	116.32
		280.7				33.2			
		329.4				104.6			
103	63.56	233.4	218	41.22	18.90	400.7	115	192.53	167.54
		267.0				59.0			
		200.2				0.0			
		171.7				0.0			
105	18.63	326.3	297	35.05	11.81	61.6	15	30.78	200.00
		255.4				0.0			
		280.2				0.0			
		325.5				0.0			

Table 16 (cont'd)

Mix	Total FE CV (%)	Pre FE (lb*in.)	Pre FE Average (lb*in)	Pre FE SD (lb*in)	Pre FE CV (%)	Post FE (lb*in.)	Post FE Average (lb*in)	Post FE SD (lb*in)	Post FE CV (%)
108	21.51	272.4	298	57.98	19.46	0.0	4	7.38	200.00
		297.1				0.0			
		378.4				14.8			
		243.5				0.0			
109	19.23	206.8	241	46.34	19.23	0.0	0	0.00	0.00
		222.4				0.0			
		293.7				0.0			
111	2.74	330.0	321	19.30	6.01	0.0	16	28.10	173.21
		334.7				0.0			
		299.2				48.7			
112	8.22	211.4	238	19.56	8.22	0.0	0	0.00	0.00
		252.0				0.0			
		234.6				0.0			
		253.3				0.0			
127	31.83	200.8	243	37.26	15.31	0.0	64	67.47	106.23
		258.8				134.3			
		270.4				56.2			
200	4.71	252.9	242	11.39	4.71	0.0	0	0.00	0.00
		242.5				0.0			
		230.2				0.0			
201	35.82	201.3	180	19.57	10.88	122.4	52	63.40	122.68
		163.0				0.0			
		175.3				32.6			
202	11.42	172.6	185	21.12	11.42	0.0	0	0.00	0.00
		194.9				0.0			
		162.8				0.0			
		209.3				0.0			
203	17.69	272.9	289	60.45	20.95	0.0	49	49.29	100.83
		209.6				101.7			
		338.8				14.5			
		332.8				79.4			
204	18.35	366.4	377	60.36	16.01	0.0	6	10.53	173.21
		322.6				0.0			
		441.9				18.2			
206	11.44	201.3	178	20.35	11.44	0.0	0	0.00	0.00
		167.7				0.0			
		164.6				0.0			

Table 16 (cont'd)

Mix	Total FE CV (%)	Pre FE (lb*in.)	Pre FE Average (lb*in)	Pre FE SD (lb*in)	Pre FE CV (%)	Post FE (lb*in.)	Post FE Average (lb*in)	Post FE SD (lb*in)	Post FE CV (%)
208	12.76	158.3	174	22.21	12.76	0.0	0	0.00	0.00
		-				-			
		189.7				0.0			
209 A	20.44	154.5	200	40.93	20.44	0.0	0	0.00	0.00
		212.7				0.0			
		233.4				0.0			
209 B	26.52	232.8	192	46.76	24.36	11.4	4	6.58	173.21
		141.0				0.0			
		202.0				0.0			

REFERENCES

REFERENCES

- [1] AASHTO PP 60-09 Preparation of Cylindrical Performance Test Specimens Using the Superpave Gyratory Compactor (SGC), in AASHTO PP 60-09. 2011, American Association of State Highway and Transportation Officials, Washington, D.C.
- [2] AASHTO T 166-11 Bulk Specific Gravity of Compacted Hot Mix Asphalt (HMA) Using Saturated Surface-Dry Specimens, in AASHTO T 166-11. 2011, American Association of State Highway and Transportation Officials, Washington, D.C.
- [3] AASHTO T 322-07 Determining the Creep Compliance and Strength of Hot-Mix Asphalt (HMA) Using the Indirect Tensile Test Device, in AASHTO T 322-07. 2007, American Association of State Highway and Transportation Officials, Washington, D.C.
- [4] AASHTO, "Mechanistic-Empirical Pavement Design Guide: A Manual of Practice: Interim Edition," American Association of State Highway and Transportation Officials 2008.
- [5] Adeli, H., Neural Networks in Civil Engineering: 1989–2000. Computer-Aided Civil and Infrastructure Engineering, 16: (2001)126–142
- [6] Advanced Research Associates. 2002 Design Guide: Design of New and Rehabilitated Pavement Structures, NCHRP 1-37A Project, National Cooperative Highway Research Program, National Research Council, Washington, DC. (2004)
- [7] Buttlar, W.G., Roque, R. "The Development of a Measurement and Analysis System to Accurately Determine Asphalt Concrete Properties Using the Indirect Tensile Mode," Journal of the Association of Asphalt Paving Technologists, Vol. 61, 304 – 332, 1992.
- [8] Buttlar, W.G., Roque, R. "Development and Evaluation of the Strategic Highway Research Program Measurement and Analysis System for Indirect Tensile Testing at Low Temperatures," Transportation Research Record: Journal of the Transportation Research Board, No. 1454, Transportation Research Board of the National Academies, Washington, D.C., 163-171, 1994.
- [9] Ceylan, Halil, Kasthurirangan Gopalakrishnan, and Robert L. Lytton. "Neural networks modeling of stress growth in asphalt overlays due to load and thermal effects during reflection cracking." Journal of Materials in Civil Engineering 23.3 (2010): 221-229.
- [10] Christensen D.W., Bonaquist R.F., "Evaluation of Indirect Tensile Test (IDT) Procedures for Low-Temperature Performance of Hot Mix Asphalt", NCHRP Report 530. Transportation Research Board, National Research Council, Washington, D.C., USA, 2004.
- [11] Choi, J.-H., Adams, T.M. and Bahia, H.U. (2004). "Pavement roughness modeling using back-propagation neural networks." Computer-Aided Civil and Infrastructure Engineering, Vol. 19 (4): 295-303.
- [12] Demuth, H. and Beale, M., 2004. Neural Network Toolbox for use with Matlab (User's guide). Version 4, The Mathworks, Inc., Natick, MA.

- [13] Fairbairn, E. MR, and F -J. Ulm. "A tribute to Fernando LLB Carneiro (1913–2001) engineer and scientist who invented the Brazilian test." *Materials and Structures* 35.3 (2002): 195-196.
- [14] Gandhi, T., Xiao, F.P., and Amir Khanian, S.N. "Estimating indirect tensile strength of mixtures containing anti-striping agents using an artificial neural network approach." *International Journal Pavement Research and Technology*, 2(1), (2009) 475-483
- [15] Gucunski, N. and Krstic, V.. "Backcalculation of pavement profiles from spectral-analysis-of-surface-waves test by neural networks using individual receiver spacing approach." *Transportation Research Record: Journal of the Transportation Research Board*, No. 1526: (1996) 6-13.
- [16] Hill, B., Behnia, B., Hakimzadeh, S., Buttlar, W.G., and Reis, H. Evaluation of Low-Temperature Cracking Performance of Warm-Mix asphalt Mixtures. *Transportation Research Record: Journal of the Transportation Research Board*, 2294: (2012) 81–88
- [17] Hiltunen D.R., Roque R.A., "Mechanics-Based Prediction Model for Thermal Cracking Of Asphaltic Concrete Pavements", *Journal of the Association of Asphalt Paving Technologists*, AAPT, St Paul, MN, USA, Vol. 63, 1994, p. 81-117.
- [18] Huang, B., Shu, X., and Vukosavljevic, D. (2011). "Laboratory Investigation of Cracking Resistance of Hot-Mix Asphalt Field Mixtures Containing Screened Reclaimed Asphalt Pavement," *American Society of Civil Engineers Journal of Materials in Civil Engineering*, Vol. 23, No. 11, pp. 1535-1543.
- [19] Huang, C., Najjar, Y.M. and Romanoschi, S.A. (2007). "Predicting asphalt concrete fatigue life using artificial neural network approach." *Transportation Research Board Annual Meeting*, Washington, DC.
- [20] Huang, B., Zhang, Z., and Kingery, W. (2004) "Fatigue crack characteristics of HMA mixtures containing RAP." *Proc. Fifth Int. RILEM Conf. on Cracking in Pavements*, RILEM, Bagnaux, France, 631-638.
- [21] Jung, Duhwoe, and T. S. Vinson. "Thermal stress restrained specimen test to evaluate low-temperature cracking of asphalt-aggregate mixtures." *Transportation research record* 1417 (1993).
- [22] Kim, Y. R., and H. Wen. "Fracture work from indirect tension testing." *Journal of the Association of Asphalt Paving Technologists* 71 (2002).
- [23] Kim, Y.R., King, M., and Momen, M. "Typical Dynamic Moduli Values of Hot Mix Asphalt in North Carolina and Their Prediction", CD-ROM. 84th Annual Meeting, TRB, 2005.

- [24] Li, Xue, and Marasteanu. M., "Evaluation of the Low Temperature Fracture Resistance of Asphalt Mixtures Using the Semi Circular Bend Test." *Journal of the Association of Asphalt Paving Technologists* 73 (2004).
- [25] Li, X., Marasteanu, M., Kvasnak, A., Bausano, J., Williams, R., and Worel, B. (2010). "Factors Study in Low-Temperature Fracture Resistance of Asphalt Concrete." *J. Mater. Civ. Eng.*, 22(2), 145–152.
- [26] Marasteanu, M. O., Li, X., Clyne, T.T., Voller, V.R., Timm, D.H., and Newcomb, D.E. (2004). "Low temperature cracking of asphalt concrete pavements." Rep. No. MN/RC-2004-23, Dept. of Civil Engineering, Univ. of Minnesota, Minneapolis.
- [27] Marasteanu, M., Zofka, A., Turos, M., Li, X., Velasquez, R., Li X., Buttlar, W., Paulino, G., Braham, A., Dave, E., Ojo, J., Bahia, H., Williams, C., Bausano, J., Gallistel, A., and McGraw, J. (2007). "Investigation of low temperature cracking in asphalt pavements national pooled fund study 776." Rep. No. MN/RC 2007-43, Dept. of Civil Engineering, Univ of Minnesota, Minneapolis.
- [28] Pavement ME Design Version 1.0, NCHRP 1-40 D (2007) Guide for Mechanistic-Empirical Design of New and Rehabilitated Pavement Structures, Final Report. NCHRP, National Research Council, Washington, D. C., March 2004, updated 2007.
- [29] Muench, Stephen T.. "Pavement Distress." HAPI Asphalt Pavement Guide. Hawaii Asphalt Paving Industry, n.d. Web. 10 Nov 2013.
- [30] Prowell, B., and G.C. Hurley. *Warm-Mix Asphalt: Best Practices*. NAPA Quality Improvement Series 125. National Asphalt Pavement Association, Lanham, Md., 2007
- [31] Singh, D., Zaman, M., and Commuri, S. "Evaluation of Predictive Models for Estimating Dynamic Modulus of HMA Mixtures Used in Oklahoma", 2010.
- [32] Tarefder, R.A, White, L. and Zaman, M. (2005b). "Neural network model for asphalt concrete permeability." *Journal of Materials in Civil Engineering*, Vol. 17 (1) 19-27.
- [33] Tutumluer, E. and Seyhan, U. (1998). "Neural network modeling of anisotropic aggregate behavior from repeated load triaxial tests." *Transportation Research Record: Journal of the Transportation Research Board*, No. 1615: 86-93.
- [34] Ruth, B.E., Rogue, R., and Nukunay, B. (2002) "Aggregate Gradation Characterization Factors and Their Relationship to Fracture Work and Failure Strain of Asphalt Mixtures," *Journal of the Association of Asphalt Paving Technologists*, Vol. 71, pp. 310-344
- [35] Vinson T.S., and Janoo V.C., Haas R.C.G., "Low Temperature and Thermal Fatigue Cracking", SHRP Summary Report No. A-003A, Strategic Highway Research Program, National Research Council, Washington, DC, USA, 1989.
- [36] Von Quintus, H.L., "Performance Prediction Models In the Superpave Mix Design System", SHRP Report No. A-699. Strategic Highway Research Program, National Research Council, Washington, DC. , USA, 1994.

- [37] Wagoner, Michael P., et al. "Investigation of the fracture resistance of hot-mix asphalt concrete using a disk-shaped compact tension test." *Transportation Research Record: Journal of the Transportation Research Board* 1929.1 (2005): 183-192.
- [38] Witczak, M.W, Kaloush, K., Pellinen, T., El-Basyouny, M., and Quintus, H. Simple Performance Test for Superpave Mix Design, NCHRP Report 465, 2002
- [39] Wen, Haifang. "Use of fracture work density obtained from indirect tensile testing for the mix design and development of a fatigue model." *International Journal of Pavement Engineering* ahead-of-print (2012): 1-8.
- [40] Zborowski A, Kaloush KE "A Fracture Work Approach to Model the Thermal Cracking Performance of Asphalt Rubber Mixtures," *Road Materials and Pavement Design* Vol. 12 Iss.2 2011
- [41] Zhiming S., Little D.N., and Lytton P.E., "Characterization of Microdamage and Healing of Asphalt Concrete Mixtures", *Journal of Materials in Civil Engineering*, American Society of Civil Engineers, Washington, DC, USA, 2002.